

LU-TP 20-23  
June 2020

# Mass-Singularity Structure of QED and Perturbative Quantum Gravity Scatterings

**Santiago Londoño Castillo**

Department of Astronomy and Theoretical Physics, Lund University

Bachelor thesis supervised by Roman Pasechnik and Stefan Prestel



**LUND**  
UNIVERSITY

## Abstract

In this thesis, the mass singularities occurring in the cross-section of electron scattering processes are investigated. Two types of scatterings are studied: Quantum Electrodynamics (QED) scatterings, and Perturbative Quantum Gravity (PQG) scatterings. We show how mass singularities in QED and PQG cancel when real and virtual diagrams are included in the scattering cross-section. We find that in both theories, the scattering cross-section is infrared (IR) finite and that IR singularities are regulated by the finite energy resolution of the detector. Finally, the differences in the eikonal factorization and the mass singularity structure in QED and PQG are studied. From this, some important properties of PQG are inferred and discussed.

## Popular Abstract

Throughout history, the quest to find a theory that can explain nature and all of its interactions has inspired the physics community. From the ancient Greeks and their classical four-element model to Mendeleev's periodic table, humans have always sought to understand the universe at its most fundamental level. In the 20th century, two theories that would completely revolutionize our understanding of the universe were conceived: general relativity and quantum field theory.

Formulated by Albert Einstein in 1915, general relativity describes the fundamental force of gravity as a geometric property of spacetime. General relativity allowed physicists to study the large-scale properties of the universe, such as the dynamics of planets, stars, and galaxies, and predicted the existence of gravitational waves and black holes. On the other hand, our understanding of the smallest particles and their interaction comes from a quantum field theory, the Standard Model (SM) of particle physics. The SM describes three of the four fundamental forces: the weak force, the strong force, and the electromagnetic force. The fourth force, gravity, has not yet been incorporated into the SM.

Quantum field theories are like mathematical machines that take certain information in, e.g. the energies of particles and their masses, and return quantities involving the interaction of those particles, such as the probability of a process occurring or the direction in which the particles will fly after the interaction. However, these machines can sometimes malfunction and return *singular* results, i.e. when the "machine" outputs infinite quantities. These results are unphysical since we all know that it's impossible to have particles with infinite energies or a process occurring with infinite probability. Thus, if we want a theory to make any physical sense, we must make sure such singularities do not occur.

The goal of this work is to remove some of the singularities occurring in Perturbative Quantum Gravity (PQG). PQG is one of the many attempts to incorporate gravity into the SM. Removing singularities is not important only because singularities are unphysical. The process of removing such singularities can also teach us a lot about the theory itself and its properties. By studying singularities in PQG, we hope to get one step closer to understanding gravity and its quantum properties.

# Contents

<b>1</b>	<b>Introduction</b>	<b>1</b>
<b>2</b>	<b>Mass singularities in QFT</b>	<b>2</b>
2.1	Quantum field theory and mass singularities . . . . .	2
2.2	Mass singularities in QED . . . . .	3
2.3	Electron scattering calculation . . . . .	5
2.3.1	Electron scattering cross-section . . . . .	5
2.3.2	Tree-level diagram . . . . .	5
2.3.3	Electron vertex correction . . . . .	7
2.3.4	External leg corrections . . . . .	9
<b>3</b>	<b>Singularity cancellation</b>	<b>13</b>
3.1	Soft bremsstrahlung radiation . . . . .	13
3.2	Infrared singularities . . . . .	15
3.3	Collinear singularities . . . . .	16
3.4	Cancellation beyond leading order . . . . .	17
<b>4</b>	<b>Perturbative quantum gravity</b>	<b>21</b>
4.1	Spin-2 gravitons . . . . .	21
4.2	Gravitational electron scattering . . . . .	22
<b>5</b>	<b>Conclusion</b>	<b>26</b>
<b>A</b>	<b>Feynman rules</b>	<b>28</b>
A.1	Quantum electrodynamics . . . . .	28
A.2	Perturbative quantum gravity . . . . .	29
<b>B</b>	<b>Numerator algebra</b>	<b>30</b>
<b>C</b>	<b>Supplementary calculations</b>	<b>30</b>
C.1	Tree level diagram QED . . . . .	30
C.2	Imaginary factors in propagators . . . . .	31

C.3	Soft graviton simplification . . . . .	32
<b>D</b>	<b>Integral evaluation</b>	<b>32</b>
D.1	Eq. 2.24 . . . . .	33
D.2	Eq. 2.26 . . . . .	33
D.3	Eq. 4.8 . . . . .	34
	<b>References</b>	<b>36</b>

## Acknowledgments

I would like to give special thanks to my supervisors Stefan Prestel and Roman Pasechnik for their constant help and valuable comments throughout this work. I would also like to thank my friend Eivind Jørstad for his helpful comments and all the fruitful discussions about quantum field theory.

## List of acronyms

GR	General Relativity
IR	Infrared
PQG	Perturbative Quantum Gravity
QCD	Quantum Chromodynamics
QED	Quantum Electrodynamics
QFT	Quantum Field Theory
QM	Quantum Mechanics
SCET	Soft-Collinear Effective Theory
SM	Standard Model
UV	Ultraviolet

## Notations and Conventions

- Throughout this work “natural units” have been used, i.e.  $\hbar = c = 1$ .
- The Minkowski metric tensor with metric signature  $(+, -, -, -)$  will be represented by  $\eta_{\mu\nu}$  or  $\eta^{\mu\nu}$ .
- For contractions between 4-momentum vectors and gamma matrices we will follow Feynman’s notation, where  $\not{p} \equiv \gamma^\mu p_\mu$ .
- Graviton lines in Feynman diagrams have been represented by double photon lines.
- The spacial component of 4-vectors has been represented by bold letters;  $p^\mu = (p^0, \mathbf{p})$
- In Feynman diagrams time flows vertically from bottom to top.

# 1 Introduction

Quantum Field Theory (QFT) and General Relativity (GR) constitute two of the most successful and influential scientific achievements of the 20th century. QFT combines three major fields of modern physics: special relativity, quantum mechanics (QM), and classical field theory, and it provides the theoretical framework for the treatment of elementary particles and their interactions. Hitherto, the most successful QFT is the Standard Model (SM) of particle physics, which provides a set of mathematical and pictorial techniques to describe processes involving three of the four known fundamental forces: weak, strong, and electromagnetic forces. Nonetheless, gravity has not yet been incorporated into the SM.

Although many candidates for a theory of quantum gravity - such as loop quantum gravity and superstring theory - have been devised, a full, self-consistent theory of quantum gravity has not yet been discovered. Hence, quantum gravity remains one of the most fundamental unanswered questions in theoretical physics. One of the simplest ways to describe GR in terms of a QFT is by using linearized gravity, an approximation of GR in the limit where gravity is very weak. This approach to quantum gravity is known as Perturbative Quantum Gravity (PQG). In PQG, the weak field expansion of GR is used to obtain the gravitational Lagrangian, from which the Feynman rules for graviton-graviton and graviton-matter interactions can be extracted [1].

The transition amplitude of some scattering processes can become divergent if the masses of internal particles are allowed to vanish. These singularities in the transition amplitudes are known as mass singularities. Based on their physical origin, mass singularities can be classified into two types: collinear and infrared (IR) singularities. The goal of this work is to study the structure of mass singularity cancellations in QED and PQG scatterings. The cancellation of mass singularities in PQG is important for two reasons. First of all, if PQG is to be a predictive theory, it cannot yield singular observables. That is, any mass singularities occurring in separate Feynman diagrams must cancel when observables are calculated. In QED, one of the most successful and well tested QFTs, all observables are free of mass singularities [2]. Secondly, the cancellation mechanism of mass singularities can provide important information on the kinematic properties of PQG. By comparing the cancellation mechanism of mass singularities in QED and PQG, we hope to gain a better understanding of the fundamental differences between PQG and other gauge theories.

This thesis is structured as follows: in section 2, we briefly introduce QFT, mass singularities, and the formalism and tools required for the study of scatterings. In subsection 2.3, the non-radiative diagrams relevant for the electron scattering in QED are computed explicitly. We will show that the cross-section obtained from these diagrams contains soft and collinear singularities. In section 3, the cross-section for an electron scattering with one real photon in the final state will be calculated. We will demonstrate how the IR singularities in the real radiation diagrams cancel the IR singularities in the non-radiative diagrams. At the end of section 3, the cancellation of IR singularities to all orders in QED is proven. In subsection 4.1, a brief introduction to PQG is given. Furthermore, the soft graviton



factorization will be studied and used to compute the real and virtual contributions of soft gravitons to a gravitational electron scattering. We will show, to all orders in the soft graviton approximation, that PQG electron scatterings contain no mass singularities. In section 5, the main results of the calculations are summarized and discussed. The results from section 4 will be used to discuss the mechanism that enables the cancellation of all mass singularities in PQG but not in QED.

## 2 Mass singularities in quantum field theories

In this section, the fundamentals of QFT are introduced, including the main tools for QFT computations, such as the scattering matrix (S-matrix) formalism and Feynman diagrams [3, 4, 5]. Moreover, the origin of mass singularities in QFT calculations will be discussed [3, 4, 6]. Throughout this section, QED will be used to demonstrate, by computing explicit examples, the different sources of mass singularities in scattering processes.

### 2.1 Quantum field theory and mass singularities

In quantum mechanical problems, one is often interested in the probability for a certain process to occur, e.g. the probability that an electron found at position  $x_0$  at time  $t_0$  is observed at position  $x'$  at a later time  $t'$ . The probability amplitude of this process is often calculated using the time-dependent Schrödinger equation. However, there is a fundamental complication with this approach; the solution to this problem violates causality. In other words, the probability for this process to occur is non-zero outside the particle's light cone. These types of discrepancies in the early stages of quantum mechanics led physicists to develop a relativistic formulation of quantum mechanics, QFT. QFT provides the necessary tools for relativistic quantum mechanical calculations.

At the heart of QFT lies the idea that fundamental particles - such as electrons and photons - can be treated as the excited modes of a field. The exact nature and properties of a particular quantum field are determined by the Lagrangian of that particular theory, which is usually obtained using gauge symmetry arguments. Likewise, in the QFT formalism, particle interactions - such as scatterings - correspond to interactions between the particles' quantum fields. The exact form of the interaction between fields is usually obtained using the local gauge invariance of the gauge theory. For a detailed discussion on the fundamentals of QFT, the reader is referred to references [3, 4].

One of the most extensively used tools in QFT are Feynman diagrams, which pictorially represent the time-dependent perturbative expansion of particle scatterings. Feynman diagrams are of great importance since they provide a way to approximately solve QFT problems. Given the Lagrangian of a theory, any allowed interaction can be represented

pictorially as a diagram. By following a set of rules, known as Feynman rules, the matrix element  $\mathcal{M}$ , which contains all the dynamic information of the process, can be extracted from the Feynman diagram. Then, the transition amplitude squared of a process, i.e. its cross-section, can be obtained by squaring the matrix element of the process and integrating it over the appropriate phase space of final states.

Once the Feynman diagram of a process has been drawn, the transition amplitude of the process is an analytic function in the momenta of external legs and the masses of internal lines [5]. Feynman amplitudes can yield divergent quantities - singularities - for certain values of external momenta and internal masses. Throughout this work, we will focus on **mass singularities**, i.e. singularities that occur quite independently of the external momenta [6] and are associated with vanishing masses of internal particles.

Now that the main ideas of probability amplitudes in QFT have been presented, and mass singularities have been introduced, an example of a QFT calculation containing mass singularities will be discussed in detail. The following calculation will serve to illustrate how mass singularities in cross-sections occur. This calculation will yield two different types of mass singularities: infrared singularities - also known as soft singularities - and collinear singularities. The meaning and origin of the different types of singularities will be discussed as they appear in the calculations. Given that probability amplitudes are associated with observables, the fact that such calculations can yield divergent results is a catastrophe. Therefore, it will be necessary to introduce a method to remove the appearance of divergent observables in QFT.

## 2.2 Mass singularities in QED

The strategy that we will follow to study mass singularities is to first perform the electron scattering calculation in QED and study the structure of mass singularities and their cancellation in detail in this theory. Then, by transferring the tools and understanding of mass singularities in QED to gravity, we will perform a similar calculation in the framework of PQG. We decided to work in the framework of QED since it is the simplest and most tested known physical gauge theory. Nonetheless, the techniques and concepts developed in this section can be generalized to any other gauge theory. Moreover, as we shall see later, we will be able to generalize many of the results and methods from QED to PQG. It is assumed that the reader is familiar with the Feynman rules for QED, a list of basic Feynman rules is provided in Appendix A.

The process that we will use to study mass singularities, both in QED and PQG, is the scattering of a fermion, namely an electron, off an arbitrary charged particle. In particular, we are interested in the probability amplitude of the process shown in Figure 1. To calculate this probability amplitude, we will employ the S-matrix formalism.

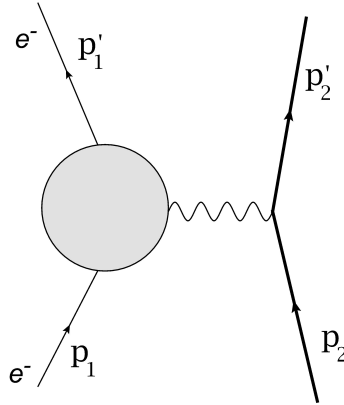


Figure 1: Feynman diagram of an electron scattering off an arbitrary charged particle. The gray circle indicates the sum of all diagrams contributing to the process.

### S-matrix formalism

In QFT, the scattering matrix - also known as S-matrix - is used to compute the transition probability from a set of initial states with definite momenta to a set of final states with definite momenta. The S-matrix is a unitary operator whose matrix elements  $S_{fi}$  are defined to be the projection of an initial state  $|\Psi_i\rangle$ , on the final state  $\langle\Psi_f|$ . Due to the unitary nature of the S-matrix, the  $T$ -matrix can be defined as follows:

$$\hat{S} = \hat{I} + i\hat{T}. \quad (2.1)$$

The  $T$ -matrix contains the “interaction” part of the S-matrix, so if the incoming particles do not interact, the S-matrix is simply the identity operator. A careful perturbative treatment of the S-matrix operator leads to the formalism of how quantum fields interact with one another and with external states, ultimately leading to Feynman diagrams. However, this treatment is outside the scope of this work, and we will state the main results without proof. The reader is referred to [4] for a more formal treatment of the subject.

The main result that we will use from the formalism of the S-matrix will be the appearance of the invariant matrix element  $\mathcal{M}$ , defined using the  $T$ -matrix as follows:

$$T_{if} = (2\pi)^4 \delta^{(4)}\left(\sum_i p_i - \sum_f p_f\right) \cdot i\mathcal{M}(p_i \rightarrow p_f), \quad (2.2)$$

where  $p_i$  and  $p_f$  stand for the 4-momenta of the incoming and outgoing particles respectively. The delta function guarantees conservation of momentum in the scattering process. The matrix element  $\mathcal{M}$  plays a similar role to the scattering amplitude  $f(\theta)$ , which most students have encountered in quantum mechanics courses. Since  $\mathcal{M}$  is defined using the  $T$ -matrix, it contains all the dynamical information of the scattering process, i.e. the physics that depends on the Hamiltonian of the particular gauge theory. The matrix element  $\mathcal{M}$  can then be obtained using Feynman diagrams as follows:

$$i\mathcal{M} = \text{Sum of all allowed Feynman diagrams}, \quad (2.3)$$

where the diagrams are evaluated according to the Feynman rules of the given theory. See Appendix A for a list of Feynman rules for QED and PQG.

## 2.3 Electron scattering calculation

### 2.3.1 Electron scattering cross-section

It can be shown, see [3], that the differential cross-section of the electron scattering process displayed in Figure 1 is given by:

$$\left(\frac{d\sigma}{d\Omega}\right)_{CM} = K|\mathcal{M}(p_1, p_2 \rightarrow p'_1, p'_2)|^2, \quad (2.4)$$

where  $K$  is a kinematic factor containing normalization constants and factors depending on the energies and 3-momenta of the external particles. For this work, the exact form of the kinematic factor will not be relevant, as it contains no mass singularities. For the matrix element squared, all non-observed degrees of freedom in the final states - such as spins and polarizations - must be summed over, while the quantum numbers in the initial state must be averaged over.

The first step to compute the cross-section of the electron scattering is to draw all Feynman diagrams that contribute to the process. Henceforth, Feynman gauge will be adopted for all the calculations, i.e.  $n = 0$  in Eq. A.4. In this work, we will only consider tree-level and one-loop order diagrams. Using the Feynman rules in Appendix A, one finds one diagram at tree-level and three first order correction diagrams that are relevant for the electron scattering process, see Figure 2. It is worth noting that due to the mass difference, radiative corrections diagrams - such as diagrams B, C, and D - involving the heavier particle are kinematically suppressed and have not been included. Vacuum polarization diagrams, i.e. diagrams containing loops in the boson propagator, have not been included either, as these diagrams only lead to a renormalization of the electric charge, with no consequences for the results of this work.

From Figure 2, the matrix element squared is given by:

$$|\mathcal{M}|^2 = |A + B + C + D|^2. \quad (2.5)$$

Noting that  $|\mathcal{M}|^2 = \mathcal{M}\mathcal{M}^*$ , we can expand the above expression, keeping only the first two leading order terms in the coupling constant  $e$ :

$$|\mathcal{M}|^2 = |A|^2 + 2\text{Re}(AB^* + AC^* + AD^*) + \mathcal{O}(e^8). \quad (2.6)$$

In the above expression,  $e = -|e|$  is the electron charge.

### 2.3.2 Tree-level diagram

Diagram  $A$  in Figure 2 is the tree-level diagram, corresponding to the simple scattering of an electron off another charged particle. The matrix element for this process can be

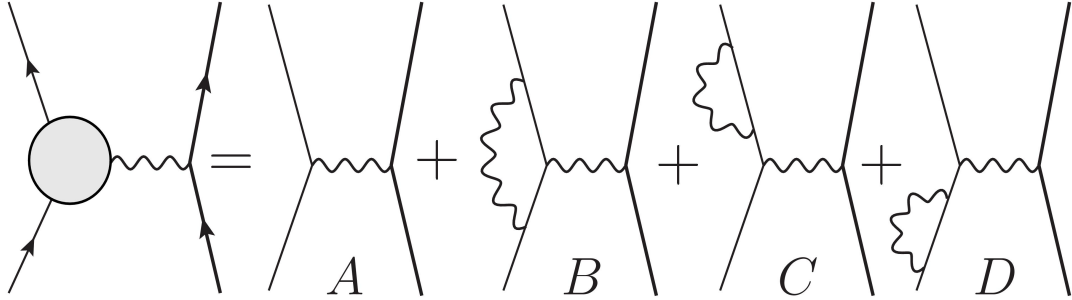


Figure 2: Tree-level diagram and first order non-radiative correction diagrams which contribute to the scattering of an electron off a heavier particle. Note that all the diagrams on the right hand side have the same final state as the diagram on the left hand side.

obtained using the Feynman rules for QED, listed in Appendix A:

$$= ie^2 \bar{u}(p'_1, s'_1) \gamma^\mu u(p_1, s_1) \frac{\eta_{\mu\nu}}{q^2} \bar{u}(p'_2, s'_2) \gamma^\nu u(p_2, s_2), \quad (2.7)$$

where  $q = p_1 - p'_1$  is the photon momentum. In Appendix C, it is shown how after simplifying the above expression, multiplying by its complex conjugate and summing over spins, the matrix element squared becomes:

$$|A|^2 = \frac{8e^4}{q^4} [(p_1 \cdot p'_2)(p'_1 \cdot p_2) + (p_1 \cdot p_2)(p'_1 \cdot p'_2) - m^2(p_1 \cdot p'_1)]. \quad (2.8)$$

This expression can be evaluated in the center-of-mass frame of the scattering process. However, we will not simplify this equation any further since we are not interested in the exact numerical cross-section of the process. Instead, we want to study mass singularities appearing in cross-sections. It is clear that Eq. 2.8 is singular only if  $q^2 = 0$ , originating from a nearly on-shell virtual photon. This singularity is not a mass singularity since it generally depends on the values of external momenta. Hence, we can conclude that the tree-level diagram contains no mass singularities. This result will turn out to be very important because as we shall see, the higher order terms in Eq. 2.6 will factorize into the tree-level part of the scattering, i.e.  $|A|^2$ , times a factor which contains all the mass singularities.

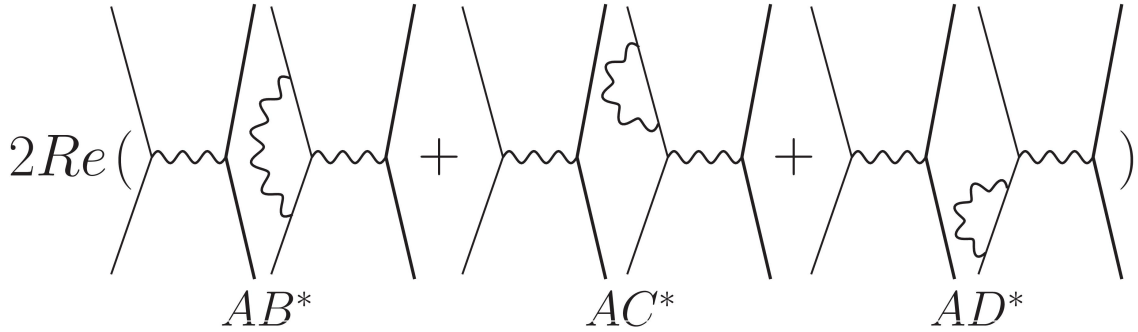


Figure 3: Diagrammatic representation of the second order correction terms to the electron scattering process.

### 2.3.3 Electron vertex correction

Equipped with the diagrams in Figure 3, we are ready to evaluate the higher order corrections in Eq. 2.6. We will begin by computing the electron vertex diagram, see diagram  $B$  in Figure 2. Using the Feynman rules for QED in Feynman gauge, i.e.  $n = 0$  in Eq. A.4, and the momentum labelling as indicated in Figure 4, the matrix element of the electron vertex correction is:

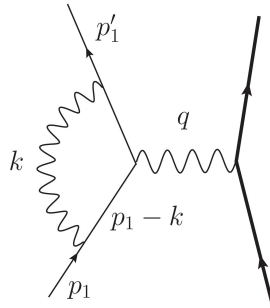


Figure 4: Feynman diagram of an electron scattering with a virtual photon connecting the two external electron legs, known as electron vertex correction.

$$B = -\bar{u}(p_1') \left[ \int \frac{d^4k}{(2\pi)^4} (-ie\gamma^\alpha) \frac{i(\not{p}_1' - \not{k} + m_1)}{[(p_1' - k)^2 - m_1^2 + i\epsilon]} \frac{-i\eta_{\alpha\beta}}{[k^2 + i\epsilon]} \frac{i(\not{p}_1 - \not{k} + m_1)}{[(p_1 - k)^2 - m_1^2 + i\epsilon]} (-ie\gamma^\beta) \right] \mathcal{A}_0,$$

where  $\mathcal{A}_0$  has been defined such that  $A = \bar{u}(p_1')\mathcal{A}_0$ , where  $A$  is the matrix element of the tree-level diagram. Using the identities in Appendix B, the numerator and denominator of the above expression can be greatly simplified, giving:

$$B = \frac{-2ie^2}{(2\pi)^4} \left[ \int d^4k \frac{2((p'_1 \cdot p_1) + k^2) - ((k \cdot p'_1) + (k \cdot p_1))}{(k^2 - 2p'_1 \cdot k + i\epsilon)(k^2 + i\epsilon)(k^2 - 2p_1 \cdot k + i\epsilon)} \right] A. \quad (2.9)$$

Eq. 2.9 yields a very important result; the matrix element of the vertex diagram factorizes into a kinematic factor, which depends only on the momenta of the different particles, times the tree-level matrix element  $A$ . The kinematic factor in Eq. 2.9 contains three singularities. To display the singularities in the integral without explicitly solving it, light-cone coordinates will be used to represent the momenta of the particles.

### Light-cone coordinates

Any 4-vector can be decomposed in light-cone components as follows:

$$p^\mu = \frac{1}{2}(\bar{n} \cdot p)n^\mu + \frac{1}{2}(n \cdot p)\bar{n}^\mu + p_\perp^\mu, \quad (2.10)$$

where  $n^\mu$  and  $\bar{n}^\nu$  are light-like vectors such that  $n^\nu n_\nu = \bar{n}^\nu \bar{n}_\nu = n^\nu p_{\perp\nu} = \bar{n}^\nu p_{\perp\nu} = 0$  and  $n^\nu \bar{n}_\nu = 2$ . Defining  $p_+ \equiv \bar{n} \cdot p$  and  $p_- \equiv n \cdot p$ , the invariant mass of a 4-vector in terms of its light-cone components is given by:

$$p^2 = (n \cdot p)(\bar{n} \cdot p) + p_\perp^2 = p_+ p_- + p_\perp^2. \quad (2.11)$$

In this work, we are mainly concerned with singularities occurring in the limit where particles become soft or collinear to other particles. Therefore, we would like to have a clear, mathematical definition of what we mean by a particle being *soft* or *collinear*. The light-cone decomposition allows us to scale the components of a 4-vector so that it behaves as a soft particle or a collinear particle. Throughout this work, we will borrow the component-scaling scheme used in the soft-collinear effective theory (SCET) for QCD [7]. To study the behavior of a collinear particle in the direction  $n_\nu$ , the **collinear scaling** of the light-cone components will be used. The collinear scaling is defined as:

$$p^\mu = \{p_+, p_-, p_\perp\} \sim \{1, \lambda^2, \lambda\}. \quad (2.12)$$

Similarly, the **soft scaling** is defined by the following scaling of the components:

$$p^\mu = \{p_+, p_-, p_\perp\} \sim \{\lambda, \lambda, \lambda\}. \quad (2.13)$$

The desired scaling is achieved by letting  $\lambda$  go to zero. Note that in both scaling schemes, the invariant mass of  $p$  goes to zero as  $\sim \lambda^2$ , meaning that we are working in the ultra-relativistic limit of  $p$ .

Now that light-cone decomposition has been defined, let us rewrite Eq. 2.9 in light-cone components by setting  $p'_1$  in the direction of  $n$ , as follows:

$$p'_1 = |p'_1|n; \quad k = \frac{1}{2}k_+n + \frac{1}{2}k_-\bar{n} + k_\perp; \quad p_1 = \frac{1}{2}p_{1+}n + \frac{1}{2}p_{1-}\bar{n} + p_{1\perp}, \quad (2.14)$$

$$\begin{aligned} &\Rightarrow p'_1 \cdot p_1 = |p'_1|p_{1-}; \quad p'_1 \cdot k = |p'_1|k_-; \\ k \cdot p_1 &= \frac{1}{2}k_+p_{1-} + \frac{1}{2}k_-p_{1+} + k_\perp p_{1\perp}; \quad k^2 = k_+k_- + k_\perp^2. \end{aligned}$$

Using the above relations, the term inside the brackets in Eq. 2.9 becomes:

$$\int dk_+ dk_- dk_\perp^2 \frac{2(|p'_1|p_{1-} + k_+k_- + k_\perp^2) - (|p_1|k_- + \frac{1}{2}k_+p_{1-} + \frac{1}{2}k_-p_{1+} + k_\perp p_{1\perp})}{(k^2 - 2|p'_1|k_-)(k^2)(k^2 - k_+p_{1-} - k_-p_{1+} - 2k_\perp p_{1\perp})}. \quad (2.15)$$

Now, the soft scaling, as described in Eq. 2.13, can be used to study the soft behaviour of  $k$  in the above integral. Power counting in  $\lambda$  shows that while the numerator becomes constant, the denominator goes to 0 as  $\sim \lambda^4$ . This means that the integral diverges logarithmically in the limit  $\lambda \rightarrow 0$ . This type of mass singularity is known as *infrared singularity* or *soft singularity*. It occurs when the energy of the photon vanishes or becomes arbitrarily small. This means that the matrix element of the vertex diagram becomes arbitrarily large if a virtual photon with vanishingly small energy is exchanged between the external electron legs.

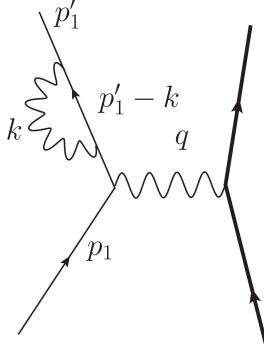
The second type of singularity present in Eq. 2.9 is a collinear singularity. Performing another power counting, this time using the collinear scaling in Eq. 2.14, one finds that while the numerator becomes a constant, the denominator inside the integral goes to 0 as  $\sim \lambda^4$ . This means that the integral is logarithmically divergent in the limit  $\lambda \rightarrow 0$ . This limit corresponds to the photon being emitted nearly collinearly to the momentum of the outgoing electron  $p'_1$ . Notice that unlike the case of the soft photon, the third parenthesis in the denominator of the above integral does not identically vanish. The same type of singularity is found if the photon is now set to be collinear to  $p_1$ .

Eq. 2.9 contains two very important properties of the vertex function: the factorization of the matrix element of the vertex diagram into a kinematic term, times the matrix element of tree-level diagram  $A$ , and the divergent behaviour of the matrix element in the soft and collinear limits.

### 2.3.4 External leg corrections

We will now compute the matrix element of diagram C in Figure 2, known as a leg correction diagram. Using the Feynman rules for QED in Appendix A, the matrix element for diagram C is:





$$\Rightarrow C = \bar{u}(p'_1)\Sigma(p'_1)\frac{(\not{p}'_1 + m_1)}{p'_1{}^2 - m_1^2 + i\epsilon}\mathcal{A}_0, \quad (2.16)$$

where  $\Sigma(p)$  is the electron self-energy. To second order in the electron charge  $e$ ,  $\Sigma$  is given by:

$$\Sigma_2(p'_1) = i(-ie\gamma^\alpha) \int \frac{d^4k}{(2\pi)^4} \frac{-i\eta_{\alpha\beta}}{(k^2 + i\epsilon)} \frac{i((\not{p}'_1 - \not{k}) + m_1)}{((p'_1 - k)^2 - m_1^2 + i\epsilon)} (-ie\gamma^\beta). \quad (2.17)$$

Eq. 2.17 can be simplified using the identities in Appendix B, giving:

$$\Sigma_2(p'_1) = \frac{-2ie^2}{(2\pi)^4} \int d^4k \frac{\not{p}'_1 + \not{k}}{(k^2 + i\epsilon)(k^2 - 2p'_1 \cdot k + i\epsilon)}. \quad (2.18)$$

Using light-cone coordinates and setting  $p'_1$  in the direction of the light-like vector  $n$ ,  $\Sigma_2(p'_1)$  becomes:

$$\Sigma_2(p'_1) = \frac{-2ie^2}{(2\pi)^4} \int dk_- dk_+ dk_\perp \frac{\not{p}'_1 + \not{k}}{(k_+ k_- + k_\perp^2)(k_+ k_- + k_\perp^2 - 2|p'_1|k_-)}. \quad (2.19)$$

Now, we would like to study the soft and collinear behavior of the electron self-energy. Using the soft scaling in Eq. 2.13 and performing a power counting, one finds that in the limit  $\lambda \rightarrow 0$ , the denominator in Eq. 2.19 goes to 0 as  $\sim \lambda^3$ . Therefore, we find that the electron self-energy contains no IR (soft) singularities.

On the other hand, performing a power counting using the collinear scaling in Eq. 2.12, one finds that the numerator in Eq. 2.19 goes to 0 as  $\sim \lambda^4$ . Hence,  $\Sigma_2$  contains a logarithmic collinear divergence, similar to the one in the electron vertex diagram, see Eq. 2.9.

Now, we would like the matrix element  $C$  to factorize into the tree-level matrix element  $A$ , times some factors, just as the electron vertex matrix element. Using Eq. B.2 to replace the numerator of the fermion propagator by a spin sum, and after some simplifications, the matrix element of the external leg correction becomes:

$$C = \frac{\not{p}'_1}{p'_1{}^2 + i\epsilon} \Sigma_2(p'_1) A, \quad (2.20)$$

where we have assumed the limit of the massless electron.

The calculation of the matrix element of the second external leg correction in Figure 2 follows the same steps as the previous calculation. Since no new physics is introduced we will simply state the result:

$$D = \frac{\not{p}_1}{p_1{}^2 + i\epsilon} \Sigma_2(p_1) A. \quad (2.21)$$

Now that the matrix elements of all the diagrams in Figure 2 have been calculated, we are in a position to compute the matrix element squared  $|\mathcal{M}|^2$  in Eq. 2.6. Taking the complex conjugate of Eq. 2.9, Eq. 2.20, and Eq. 2.21 and substituting in Eq. 2.6, one finds:

$$|\mathcal{M}|^2 = |A|^2 \left( 1 + 2\text{Re} \left[ V_f + \frac{p'_1}{p_1'^2 + i\epsilon} \Sigma_2(p'_1) + \frac{i p_1}{p_1^2 + i\epsilon} \Sigma_2(p_1) \right] \right), \quad (2.22)$$

where  $V_f$  is the kinematic vertex factor:

$$V_f = \frac{-2ie^2}{(2\pi)^4} \left[ \int d^4k \frac{2((p'_1 \cdot p_1) + k^2) - ((k \cdot p'_1) + (k \cdot p_1))}{(k^2 - 2p'_1 \cdot k + i\epsilon)(k^2 + i\epsilon)(k^2 - 2p_1 \cdot k + i\epsilon)} \right]. \quad (2.23)$$

We have seen that  $V_f$  diverges in the soft and collinear limits and that all the other terms inside the Re function in Eq. 2.22 are singular in the collinear limit. This means that unless the singularities are purely imaginary, so that their real part vanishes, the matrix element squared  $|\mathcal{M}|^2$  of the electron scattering is singular in the IR (soft) and collinear limits.

To solve the divergent integrals, which generally do not have simple analytic solutions, we will need to make some simplifications. Henceforth, an upper cutoff  $\Lambda$  on the virtual photon energy  $k^0$  will be imposed. The cutoff has been chosen so that we are only dealing with soft photons, with energies lower than the electron energies. The treatment of hard-collinear particles, which requires ultraviolet (UV) considerations, is outside the scope of this work. The soft photon approximation allows us to drop terms containing  $k$  that appear in the numerators of the integrals. Moreover, from this point forth, only the leading order of the divergent integrals will be considered. Although it is possible to keep track of all divergent order terms, the mathematics becomes increasingly complicated and the expressions become almost impossible to deal with by hand. Nonetheless, the results of the cancellation of leading order divergences contains the same physical features as a more general cancellation. Using these approximations, the divergent integrals become:

$$I_{loop} = \frac{ie^2}{(2\pi)^4} \int d^4k \frac{1}{(k^2 + i\epsilon)(p \cdot k + i\epsilon)}, \quad (2.24)$$

$$V_f = \frac{-ie^2}{(2\pi)^4} \left[ \int d^4k \frac{p'_1 \cdot p_1}{(p'_1 \cdot k + i\epsilon)(k^2 + i\epsilon)(p_1 \cdot k + i\epsilon)} \right]. \quad (2.25)$$

Before evaluating these integrals, there is a problem with our expression for the vertex function diagram, Eq. 2.9, that we first must solve. From the S matrix formalism discussed at the beginning of this section, the matrix element for the electron scattering process is given by  $\mathcal{M} = A + \delta F_1(q^2)$ . Where  $F_1$  is a form factor, which to first order is given by  $\gamma^\mu$  and to second order is determined by the vertex factor  $V_f$ . The external leg corrections do not affect the form factor since such diagrams are not one-particle irreducible, see [3] for more details. Moreover, from experimental data, we expect radiative corrections to  $F_1$  to vanish for  $q^2 = 0$ , i.e.  $\delta F_1(0) = 0$ . Thus, to satisfy this condition, the radiative correction  $\delta F_1(q^2)$  can be redefined as follows  $\delta F_1(q^2) \rightarrow \delta F_1(q^2) - \delta F_1(0)$ . Concretely, for the electron scattering process in Figure 2 the condition  $q^2 = 0$  occurs when  $p_1 = p'_1$ . Using this argument, the electron vertex correction is redefined as:

$$V_f = \frac{-ie^2}{(2\pi)^4} \left[ \int d^4k \frac{p'_1 \cdot p_1}{(p'_1 \cdot k + i\epsilon)(k^2 + i\epsilon)(p_1 \cdot k + i\epsilon)} - \frac{p_1^2}{(k^2 + i\epsilon)(p_1 \cdot k + i\epsilon)^2} \right]. \quad (2.26)$$

This new expression for  $V_f$  ensures that the correction of the vertex factor to the form factor  $F_1$  vanishes for  $q^2 = 0$ .

We are now in a position to evaluate the integrals in Eq. 2.24 and Eq. 2.26. Because of the Re function in Eq. 2.22, we are only interested in the real contribution of Eq. 2.24 and Eq. 2.26. Noting the factor of  $i$  behind both integrals, the real part comes entirely from the imaginary contributions of the integrals. In subsection C.2, it is shown that the imaginary part of such propagators arises entirely from values of  $k$  for which the terms in the denominator vanish. In Appendix D, the real contributions of the integrals in Eq. 2.24 and Eq. 2.26 are shown to be:

$$\text{Re}(I_{loop}) = \frac{\alpha}{(2\pi)^2} \int_{|\mathbf{k}_{min}|}^{\Lambda} d|\mathbf{k}| \int \Omega_{\hat{\mathbf{k}}} \frac{1}{(p^0 - \mathbf{p} \cdot \hat{\mathbf{k}})}, \quad (2.27)$$

$$\text{Re}(V_f) = \frac{-\alpha}{2\pi} \ln \left( \frac{\Lambda}{|\mathbf{k}_{min}|} \right) \left[ \frac{1}{2\beta} \ln \left( \frac{1+\beta}{1-\beta} \right) - 1 \right], \quad (2.28)$$

where  $\beta$  is the relative velocity between the incoming and outgoing electron:

$$\beta = \sqrt{1 - \frac{m_1^2 m_1'^2}{(p_1 \cdot p_1')^2}}. \quad (2.29)$$

For a massless electron, i.e.  $p^0 = |\mathbf{p}|$ , the first integral is divergent in the collinear limit  $\mathbf{p} \cdot \hat{\mathbf{k}} = |\mathbf{p}|$ . The second integral diverges in the soft limit  $|\mathbf{k}_{min}| \rightarrow 0$ . Furthermore, letting the mass  $m_1$  of one of the particles go to zero while fixing its momentum  $\mathbf{p}$  constant, one can Taylor expand  $\beta$  and show that the second integral is also divergent, corresponding to a collinear singularity. This shows that the matrix element squared of the electron scattering diverges both in the soft limit and in the collinear limit. Since the matrix element squared is related to an observable quantity, i.e. the cross-section of the scattering process by Eq. 2.4, it should not contain singularities.

Before we provide a method to remove mass singularities, let us try to interpret the results of our calculations. First of all, note that unlike the singularity present in the tree-level diagram, see Eq. 2.8, mass singularities found in this section occur independently of the values of the momenta of the external legs and depend exclusively on the energy of the virtual photon and its relative orientation with respect to the external legs. This is consistent with the definition of mass singularities provided at the beginning of this section. The name *mass singularities* derives from the fact that these singularities are associated with the vanishing masses of particles. The simplest way to see this is by noting that IR (soft) singularities can be regularized by introducing a non-zero photon mass  $m_\gamma$ . With

this fictitious photon mass, the denominator in the logarithm in Eq. 2.28 does not vanish, and the matrix element is no longer singular. Similarly, because the momentum of a massive particle cannot be light-like, collinear singularities are regulated by the non-vanishing electron mass  $m_e$ .

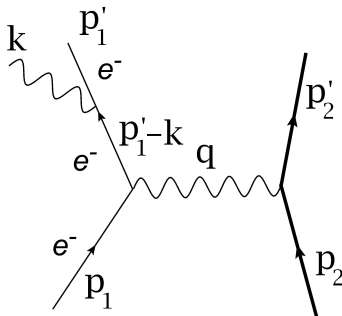
There is one more singularity associated with all diagrams containing virtual corrections which we have not discussed so far; ultraviolet singularities, which occur due to the integration over the virtual photon momentum  $d^4k$ , whose upper limit needs not to be finite. However, it will be assumed that all UV singularities have been regularized by adding appropriate counterterms. UV regularization will not affect any of the methods or results discussed in this or the following sections.

### 3 Cancellation of mass singularities in QED

In this section, we will show how some of the mass singularities discussed in the previous section cancel to first order when the contribution of **real radiation** diagrams, such as the ones shown in Figure 5, are included in the calculation of the matrix element of the electron scattering. Moreover, by following a similar approach to Weinberg's in reference [8], we will show the cancellation of infrared singularities in QED to all orders. At the end of this section, we will discuss why it is relevant and consistent to include real radiation diagrams in the calculation of the cross-section of the electron scattering in Figure 1.

#### 3.1 Soft bremsstrahlung radiation

In classical electrodynamics, it is well known that a charged particle undergoing an acceleration will radiate photons, a process that is known as **bremsstrahlung**. Analogously, in QED, a charged particle can emit a photon, as long as energy and momentum are conserved. The process that we will study in this section is the radiation of a soft photon during the scattering of an electron from a heavier particle, i.e.  $xe^- \rightarrow \gamma xe^-$ . To first order, the Feynman diagrams contributing to this process are shown in Figure 5. Using the Feynman rules in Appendix A, the matrix element of the diagram on the left of Figure 5 gives:



$$\Rightarrow \bar{u}(p'_1)(-ie\gamma^\mu)\epsilon_\mu^*(k)\frac{i((\not{p}'_1 - \not{k}) + m_1)}{(p'_1 - k)^2 - m_1^2 + i\epsilon}\mathcal{A}_0. \quad (3.1)$$

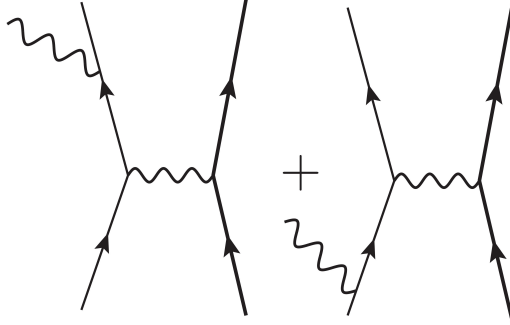


Figure 5: Feynman diagrams of electron scattering with real radiation. The matrix element of these diagrams becomes singular in the soft radiation limit or in the limit where a massless electron emits a collinear photon.

Now, let us simplify the above expression by assuming a soft photon, so that the term  $\not{k}$  in the numerator can be dropped. Using the identities in Appendix B, Eq. 3.1 can be greatly simplified in the soft photon approximation, giving:

$$R_1 = e \frac{2p'_1 \cdot \epsilon^*}{-2p'_1 \cdot k} \bar{u}(p'_1) \mathcal{A}_0 = e \left[ \frac{-p'_1 \cdot \epsilon^*}{p'_1 \cdot k} \right] A. \quad (3.2)$$

Similar to the factorization of the virtual corrections, the matrix element of soft bremsstrahlung factorizes into a kinematic factor, times the non-radiative tree level matrix element  $A$ . This factorization is known as the **eikonal** factorization. The eikonal factor can be shown to be quite independent of the spin of the emitting particle. However, its exact structure is determined by the conserved charges of the gauge theory being studied. As we shall see in section 4, the form of the eikonal factor in PQG will be responsible for the distinctive structure of the cancellation of mass singularities in linearized gravity.

The calculation for the matrix element of the second diagram in Figure 5 follows the same steps as the calculation above so we will not repeat it. The matrix element for soft bremsstrahlung from the incoming electron becomes:

$$R_2 = e \left[ \frac{p_1 \cdot \epsilon^*}{p_1 \cdot k} \right] A. \quad (3.3)$$

Thus, the matrix element for soft bremsstrahlung is given by:

$$R = e \left( \frac{p_1 \cdot \epsilon^*}{p_1 \cdot k} - \frac{p'_1 \cdot \epsilon^*}{p'_1 \cdot k} \right) A. \quad (3.4)$$

Finally, we would like to compute the matrix element squared for soft bremsstrahlung. Thus, the above expression must be multiplied by its complex conjugate. Since there is a photon in the final state, we must sum over its polarization, and integrate over its 4-momentum. However, the emitted photon must be on-shell, therefore, a delta function

$\delta(k^2)$  must be included in the integration;

$$|R|^2 = |A|^2 e^2 \int \frac{dk^4}{(2\pi)^4} \sum_{\epsilon \text{ polarization}} \left( \frac{p_1^\mu \epsilon_\mu^* \epsilon_\nu p_1^\nu}{(p_1 \cdot k)^2} + \frac{p_1'^\mu \epsilon_\mu^* \epsilon_\nu p_1'^\nu}{(p_1' \cdot k)^2} - 2 \frac{p_1^\mu \epsilon_\mu^* \epsilon_\nu p_1'^\nu}{(p_1 \cdot k)(p_1' \cdot k)} \right) \delta(k^2). \quad (3.5)$$

The above expression can be greatly simplified by performing the sum over photon polarizations using the **Ward identity**. The Ward identity states that an arbitrary QED process - denoted by  $\mathcal{M}^\mu(k)$  - involving an external photon with momentum  $k$ , vanishes if the polarization vector  $\epsilon_\mu(k)$  is replaced by  $k$ :

$$k_\mu \mathcal{M}^\mu = 0. \quad (3.6)$$

Using the Ward identity, one can show that the sum over external photon polarizations can be replaced by the metric tensor, i.e.  $\sum \epsilon_\mu^* \epsilon_\nu \rightarrow -\eta_{\mu\nu}$ . Replacing the photon polarization sum and integrating over the first component of the photon 4-momentum using the delta function with  $k^0 = |\mathbf{k}|$ , Eq. 3.5 becomes:

$$|R|^2 = |A|^2 e^2 \int \frac{dk^3}{(2\pi)^3} \frac{1}{2|\mathbf{k}|} \left( 2 \frac{p_1 \cdot p_1'}{(p_1 \cdot k)(p_1' \cdot k)} - \frac{p_1^2}{(p_1 \cdot k)^2} - \frac{(p_1')^2}{(p_1' \cdot k)^2} \right). \quad (3.7)$$

This is almost identical to the integral we encountered when computing the real contribution of the vertex function  $V_f$ . Using the result of the known integral in subsection D.2, Eq. 3.7 becomes:

$$|R|^2 = |A|^2 \frac{\alpha}{2\pi} \ln \left( \frac{|\mathbf{k}_{max}|}{|\mathbf{k}_{min}|} \right) \left[ \frac{1}{\beta} \ln \left( \frac{1+\beta}{1-\beta} \right) - 2 \right]. \quad (3.8)$$

This expression looks very similar to the vertex function  $V_f$  from the previous section, and just like the vertex function, it also diverges in the soft and collinear limits. The meaning of  $|\mathbf{k}_{max}|$  will soon become clear, all we know right now is that it must be small enough so that the soft photon approximation still holds.

## 3.2 Infrared singularities

Hitherto, the method used to compute the matrix element of a process was to add up the contribution of all diagrams with identical final states at fixed order. In the case of the electron scattering process, we looked at the diagrams relevant to the process  $xe^- \rightarrow xe^-$  in Figure 2. Now, we will justify why electron scatterings with soft real radiation - Figure 5 - must be included in the calculation of the cross-section of the process  $xe^- \rightarrow xe^-$ .

Imagine a detector with a threshold energy resolution  $E_t$ , so that it cannot resolve energies lower than  $E_t$ . Now, consider an electron scattering process with a real photon with energy lower than  $E_t$ . To this detector, the scattering process looks like a  $xe^- \rightarrow xe^-$  process and

not like a  $xe^- \rightarrow x\gamma e^-$  process, since the detector cannot detect the final photon nor the energy missing from the final state particles. Hence, if only the two final state particles are detected, it is impossible to tell if the scattering process occurred with the emission of a soft photon with energy lower than  $E_t$  or if it was a non-radiative scattering, such as the ones in Figure 2. This means that for the calculation of the cross-section of the process  $xe^- \rightarrow xe^-$ , we must also include diagrams with real radiation that we could not resolve, i.e. processes with real radiation with energy lower than the detector's threshold  $E_t$ .

$$|\mathcal{M}_{xe^- \rightarrow xe^-}|^2 = |\mathcal{M}_{xe^- \rightarrow xe^-}^{\text{non-radiative}}|^2 + |\mathcal{M}_{xe^- \rightarrow \gamma xe^-}^{\text{soft}}|^2, \quad (3.9)$$

where the non-radiative matrix element was calculated in subsection 2.3 - see Eq. 2.22 - and the soft part is given by the the matrix element of scatterings with soft real radiation with energy lower than  $E_t$ , see Eq. 3.8. Substituting Eq. 2.24 and Eq. 2.28 in Eq. 2.22, the above equation becomes:

$$|\mathcal{M}_{xe^- \rightarrow xe^-}|^2 = |A|^2 \left\{ 1 + 4\text{Re}(I_{loop}) + \frac{\alpha}{2\pi} f(\beta) \left[ \ln \left( \frac{E_t}{|\mathbf{k}_{min}|} \right) - \ln \left( \frac{\Lambda}{|\mathbf{k}_{min}|} \right) \right] \right\},$$

$$|\mathcal{M}_{xe^- \rightarrow xe^-}|^2 = |A|^2 \left\{ 1 + 4\text{Re}(I_{loop}) + \frac{\alpha}{2\pi} f(\beta) \ln \left( \frac{E_t}{\Lambda} \right) \right\}, \quad (3.10)$$

where  $f(\beta)$  is defined as:

$$f(\beta) = \left[ \frac{1}{\beta} \ln \left( \frac{1+\beta}{1-\beta} \right) - 2 \right]. \quad (3.11)$$

Note that  $|\mathbf{k}_{min}|$  does not appear in the matrix element any longer. Moreover, all the terms in Eq. 3.10 are finite in the soft limit. Hence, we have shown how by adding the contributions of virtual and soft real photons, the IR singularities in the electron scattering cross-section cancel out to first order. In fact, the cancellation shown here is just an example of the more general *Bloch-Nordsieck theorem* [2]. This theorem states that all infrared singularities in QED with a massive electron will cancel when summing over final state radiation, as long as there is a finite energy resolution  $E_t$ .

### 3.3 Collinear singularities

Despite Eq. 3.10 being IR finite, it is still divergent in the collinear limit. In the limit of a massless electron emitting a collinear photon, both  $I_{loop}$  and  $f(\beta)$  become singular. Even worse, unlike IR singularities, collinear singularities from the real and virtual contributions do not cancel each other. The reason why collinear singularities do not cancel in our final matrix element is due to the approximations made to treat soft photons. A more careful treatment of the integrals keeping all factors of  $k$  in the numerators would lead to the cancellation of collinear singularities to first order in the final matrix element [5].

Collinear singularities in QED are generally regularized by the non-vanishing electron mass. Nonetheless, studying the behavior of collinear singularities is still relevant. Consider, for

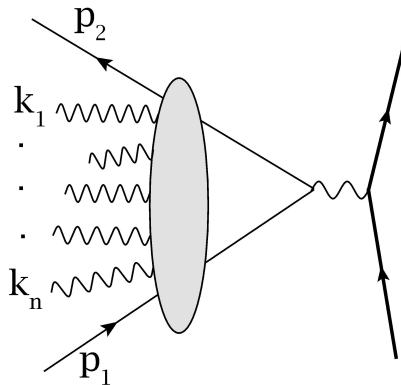


Figure 6: Feynman diagram of an electron scattering containing  $n$  soft photons connected in any possible arrangement to the external electron legs. The photons may be soft real or soft virtual photons.

instance, an experiment where the energy of the collision  $Q$  is far greater than the electron mass  $m_e$ . In such an experiment, the contribution from the collinear singularities associated with the vanishing electron mass would become important. However, Kinoshita [6], Lee, and Nauenberg [9] showed that in any unitary theory - such as QED - all mass singularities associated with the final state must cancel when integrated over all degenerate final states (**KLN theorem**). So even for ultra-relativistic electron scatterings, where the electron mass is negligible, the cross-section of the scattering process remains finite. Similarly to how IR singularities are regulated by the detector's finite energy resolution  $E_t$ , collinear singularities are regulated by the detector's finite angular resolution  $\theta_t$ , i.e. the minimum transverse component of the momentum that can be resolved. The finite angular resolution means that scatterings with real collinear photons that could not be detected must also be included in the matrix element. Including these diagrams in the calculation of the matrix element leads to the cancellation of collinear singularities, analogous to the cancellation discussed in the previous section.

### 3.4 Cancellation beyond leading order

Now that we have seen how IR singularities in an electron scattering process cancel to first order, we would like to see if this cancellation occurs beyond the first order. In this section, following a similar approach to the more general proof by Weinberg [8], we will prove the cancellation of IR singularities to all orders in an electron scattering process in QED.

Consider an electron scattering process involving an arbitrary number of soft real or virtual photons, see Figure 6. From subsection 3.1, we know that the matrix element for attaching a soft photon to the outgoing electron leg of an electron scattering process is given by Eq. 3.2 (without the photon polarization factor).

Now, consider attaching  $n$  soft photons to the outgoing electron leg. Given that the



final electron has momentum  $p'_1$ , the fermion propagator before the emission of the last photon has momentum  $p'^{(1)} \equiv p'_1 + k_1$ , the propagator before has momentum  $p'^{(2)} \equiv p'_1 + k_1 + k_2$ , until the last propagator - the one attached to the scattering vertex - has momentum  $p'^{(n)} \equiv p'_1 + k_1 + k_2 + \dots + k_n$ . Following the same simplification steps used in subsection 3.1, it is not difficult to show that the matrix element for attaching  $n$  soft photons to the outgoing electron becomes:

$$x = \bar{u}(p'_1) e^n \left( \frac{p'^{(1)}}{p'_1 \cdot k_1} \right) \left( \frac{p'^{(2)}}{p'_1 \cdot (k_1 + k_2)} \right) \dots \left( \frac{p'^{(n)}}{p'_1 \cdot (k_1 + k_2 + \dots + k_n)} \right) \mathcal{A}_0. \quad (3.12)$$

For simplicity, we will not only work in the approximation where all photons are soft, but we will also assume that the sum of all soft photons is soft. This condition allows us to make the approximation that all intermediate fermion propagators are nearly on-shell and have similar ‘‘off-shellness’’. Now, let us sum over the  $n!$  number of permutations of the ordering of the soft photons. A short proof by induction, see [3], gives that the sum of  $x$  over the different photon permutations is:

$$X = e^n \left( \frac{p'^{(1)}}{p'_1 \cdot k_1} \right) \left( \frac{p'^{(2)}}{p'_1 \cdot k_2} \right) \dots \left( \frac{p'^{(n)}}{p'_1 \cdot k_n} \right) A. \quad (3.13)$$

Now, we would like to repeat this process but instead, attach  $n$  soft photons to the incoming electron. This time, we know the initial momentum of the electron to be  $p_1$ , so that the first propagator after the soft first emission has momentum  $p_1^{(1)} \equiv p_1 - k_1$ , the second one has momentum  $p_1^{(2)} \equiv p_1 - k_1 - k_2$ , etc. The expression for the matrix element of this process is identical to Eq. 3.13, however, there is an additional minus sign inside each parenthesis, since  $(p_1 - k_i)^2 - m^2 \approx -2p_1 \cdot k_i$ . Hence, if we attach  $n$  photons to the external legs in any possible way and then sum over all the possible permutations, the following matrix element is obtained:

$$\mathcal{M} = A e^n \left( \frac{p'^{(1)}}{p'_1 \cdot k_1} - \frac{p^{(1)}}{p_1 \cdot k_1} \right) \left( \frac{p'^{(2)}}{p'_2 \cdot k_2} - \frac{p^{(2)}}{p_2 \cdot k_2} \right) \dots \left( \frac{p'^{(n)}}{p'_n \cdot k_n} - \frac{p^{(n)}}{p_n \cdot k_n} \right). \quad (3.14)$$

We have not yet specified whether these soft photons are real - bremsstrahlung - or virtual, connected to the external legs in any possible way, i.e. external leg corrections or vertex diagrams. Now, note that we can construct a virtual photon by choosing two photons  $i, j$ , setting their momenta to be  $k_i = -k_j$ , i.e. one of the photons is being emitted and the other being absorbed, inserting a photon propagator in between and integrating over the 4-momentum of the photon:

$$X_{virtual} = e^2 \int \frac{d^4 k}{(2\pi)^4} \left( \frac{p_1'^{\mu}}{p'_1 \cdot k} - \frac{p_1^{\mu}}{p_1 \cdot k} \right) \frac{-i\eta_{\mu\nu}}{k^2} \left( -\frac{p_1'^{\nu}}{p'_1 \cdot k} + \frac{p_1^{\nu}}{p_1 \cdot k} \right). \quad (3.15)$$

Where the factors of  $i\epsilon$  have been omitted to improve readability. This leads to:

$$X_{virtual} = e^2 \int \frac{d^4 k}{(2\pi)^4} \frac{1}{k^2} \left( \frac{2p_1 \cdot p'_1}{(p'_1 \cdot k)(p_1 \cdot k)} - \frac{(p'_1)^2}{(p'_1 \cdot k)^2} - \frac{p_1^2}{(p_1 \cdot k)^2} \right). \quad (3.16)$$

To obtain the above expression, we have used the fact that we are considering only soft photons, thus,  $p_1^{(i)} \approx p_1'$  and  $p_1^{(i)} \approx p_1$ . Moreover, the above factor must be multiplied by  $\frac{1}{2}$  to avoid over-counting, since permuting  $i$  and  $j$  would give the same loop. Then, the matrix element for a process containing  $m$  virtual soft photons is:

$$\mathcal{M}_{virtual}^{(m)} = A \left( \frac{X_{virtual}}{2} \right)^m \frac{1}{m!}. \quad (3.17)$$

The factor  $m!$  must be included to prevent over-counting, since permuting any of the  $m$  loops would not change the matrix element. Now, we must to add up the contribution of all diagrams containing up to  $m$  virtual loops:

$$\mathcal{M}_{virtual} = \sum_0^m \mathcal{M}_{virtual}^{(m)} \stackrel{m \rightarrow \infty}{=} A \exp \left( \frac{X_{virtual}}{2} \right). \quad (3.18)$$

Hence, the matrix element squared becomes:

$$|\mathcal{M}_{virtual}|^2 = |A|^2 \exp [\text{Re}(X_{virtual})]. \quad (3.19)$$

Note that the real part of Eq. 3.16 is almost identical to the real part of the vertex function  $V_f$ , which we computed in subsection D.2. Reusing the result from subsection D.2, the real part of Eq. 3.16 is given by:

$$\text{Re}(X_{virtual}) = \frac{-\alpha}{2\pi} \ln \left( \frac{\Lambda}{|\mathbf{k}_{min}|} \right) f(\beta), \quad (3.20)$$

where  $f(\beta)$  is again given by Eq. 3.11. Inserting Eq. 3.20 into Eq. 3.19 gives:

$$\Rightarrow |\mathcal{M}_{virtual}|^2 = |A|^2 \left( \frac{|\mathbf{k}_{min}|}{\Lambda} \right)^{\frac{\alpha}{2\pi} f(\beta)}. \quad (3.21)$$

Now, let us consider a scattering where  $n$  soft real photons are emitted. The matrix element squared for the emission of  $n$  soft real photons is obtained by inserting a photon polarization vector inside each parenthesis in Eq. 3.14, multiplying it by its complex conjugate, summing over final-state photon polarizations and integrating over the on-shell momenta of all real photons:

$$|A|^2 \int d\mathcal{K} \prod_1^n \frac{e^2}{(2\pi)^3 2|\mathbf{k}_n|} \left( \frac{p_1^\mu \Theta_{\mu\nu} p_1^\nu}{(p_1 \cdot k_n)^2} + \frac{p_1'^\mu \Theta_{\mu\nu} p_1'^\nu}{(p_1' \cdot k_n)^2} - \frac{p_1'^\mu \Theta_{\mu\nu} p_1^\nu}{(p_1 \cdot k_n)(p_1' \cdot k_n)} - \frac{p_1^\mu \Theta_{\mu\nu} p_1'^\nu}{(p_1 \cdot k_n)(p_1' \cdot k_n)} \right),$$

where  $d\mathcal{K} = d^3k_1 d^3k_2 \dots d^3k_n$  is the integration over the phase-space of on-shell photons and  $\Theta_{\mu\nu}$  is the photon polarization sum. Using the Ward identity, Eq. 3.6, the polarization sums  $\Theta_{\mu\nu} = \sum \epsilon_\mu^* \epsilon_\nu$  may be replaced by  $-\eta_{\mu\nu}$ , giving:

$$|\mathcal{M}_{real}^{(n)}|^2 = \frac{|A|^2}{(2\pi)^{3n}} \int d\mathcal{K} \prod_1^n \frac{e^2}{2|\mathbf{k}_n|} \left( \frac{2p_1 \cdot p_1'}{(p_1' \cdot k_n)(p_1 \cdot k_n)} - \frac{p_1^2}{(p_1 \cdot k_n)^2} + \frac{(p_1')^2}{(p_1' \cdot k_n)^2} \right). \quad (3.22)$$

Given that photons are bosons, we must multiply the above expression by  $\frac{1}{n!}$ , as there are  $n$  - indistinguishable - bosons in the final state. We must now integrate the expression above over the photons phase-space  $d\mathcal{K}$ . To be able to compute the integral, we will assume that the energy of all soft photons is much less than the detector threshold  $E_t$ . Ideally, the integrals should be computed so that the energies of all soft photons combined is less than  $E_t$ . However, this approach makes the integrals extremely complicated and would only introduce sub-dominant corrections. Now, we integrate Eq. 3.22 by noting that each  $d^3k$  integral is identical to the integral we encountered for the bremsstrahlung in subsection 3.1, which gives:

$$|\mathcal{M}_{real}^{(n)}|^2 = \frac{|A|^2}{n!} \left[ \frac{\alpha}{2\pi} \ln \left( \frac{E_t}{|\mathbf{k}_{min}|} \right) f(\beta) \right]^n. \quad (3.23)$$

Finally, the contribution from all diagrams containing up to  $n$  real soft photons in the final state must be added:

$$|\mathcal{M}_{real}|^2 = \sum_0^n |\mathcal{M}_{real}^{(n)}|^2 \stackrel{n \rightarrow \infty}{\cong} |A|^2 \left( \frac{E_t}{|\mathbf{k}_{min}|} \right)^{\frac{\alpha}{2\pi} f(\beta)}. \quad (3.24)$$

Using Eq. 3.24 and Eq. 3.21, the matrix element squared of an electron scattering process containing an arbitrary number of soft photon virtual loops and real soft photons becomes:

$$|\mathcal{M}|^2 = |A|^2 \left( \frac{|\mathbf{k}_{min}|}{|\mathbf{k}_{max}|} \right)^{\frac{\alpha}{2\pi} f(\beta)} \left( \frac{E_t}{|\mathbf{k}_{min}|} \right)^{\frac{\alpha}{2\pi} f(\beta)} = |A|^2 \left( \frac{E_t}{\Lambda} \right)^{\frac{\alpha}{2\pi} f(\beta)}. \quad (3.25)$$

The above expression no longer depends on  $|\mathbf{k}_{min}|$ , instead it depends on the experimental energy resolution  $E_t$  and the soft-photon energy cutoff  $\Lambda$ . Thus, given that  $f(\beta)$  is IR finite, the above expression is IR finite. Similarly to the first order cancellation in section 3, the above equation is IR finite but can become divergent in the collinear limit since  $f(\beta)$  diverges if a collinear photon is emitted from a massless external leg. This can be seen if we let the mass  $m_1$  of the external leg  $p'_1$  go to zero while fixing its spatial momentum  $\mathbf{p}'_1$  constant. Taylor expanding  $\beta$  to second order in  $m_1^2$  gives:

$$f(\beta) \approx \ln(4(p'_1 \cdot p_1)) - \ln(m_1^2 m_1^2) + \mathcal{O}(m_1^6). \quad (3.26)$$

Due to the second logarithm in the above expression,  $f(\beta)$  diverges in the limit  $m_1 \rightarrow 0$ . In section 4, by repeating this calculation for the matrix element of an electron scattering in PQG, it will be shown that the matrix element is finite both in the soft and collinear massless limit.

## 4 Perturbative quantum gravity

In this section, we will give a brief overview of the theoretical framework of PQG and its associated boson; the spin-2 graviton. Moreover, we will show how mass singularities occurring in the cross-section of a gravitational electron scattering become finite when adding real and virtual contributions. As we shall see, we will be able to reuse the mathematical machinery of the previous sections by showing that gravitational scatterings factorize into the tree level diagram, times a divergent factor, similar to those that we encountered in subsection 2.3. Furthermore, it will be shown how, by canceling IR divergences to all orders - analogously to the cancellation in subsection 3.4 - the electron scattering matrix element becomes finite both in the soft and the collinear limit, unlike QED, for which additional UV considerations are necessary to cancel collinear singularities.

### 4.1 Spin-2 gravitons

QED - and more generally the whole SM - is a field theory formulated in flat space-time, where the metric is given by the Minkowski metric  $\eta_{\mu\nu}$ . In the absence of gravity, the QED Lagrangian is given by [1]:

$$\mathcal{L}_{QED} = i\bar{\psi}\gamma^\mu D_\mu\psi - m\bar{\psi}\psi - \frac{1}{4}F^{\mu\nu}F_{\mu\nu}, \quad (4.1)$$

where  $D_\mu = \partial_\mu + ieA_\mu$  is the covariant derivative of QED, and  $F^{\mu\nu} = \partial_\mu A_\nu - \partial_\nu A_\mu$  is the electromagnetic field strength tensor. The gauge invariant formulation of QED - and the SM - as described by Eq. 4.1, holds only for flat space-time, where the metric is constant and given by  $\eta_{\mu\nu}$ . However, in GR, the metric  $g_{\mu\nu}(x)$  is a dynamical variable, whose exact form is determined by the Einstein field equations [10]. PQG provides a way to partly incorporate the formalism of GR into the gauge invariance of the SM. As the name indicates, PQG is a perturbative approach, which uses the gravitational weak field limit to approximate the metric  $g_{\mu\nu}$  as follows:

$$g_{\mu\nu} = \eta_{\mu\nu} + \kappa h_{\mu\nu}, \quad (4.2)$$

where  $\kappa$  is defined using the universal gravitational constant  $G$ ,  $\kappa = \sqrt{32G}$ , and the symmetric tensor field  $h_{\mu\nu}$  denotes the deviation of the metric tensor  $g_{\mu\nu}$  from the Minkowski metric tensor  $\eta_{\mu\nu}$ . We will not derive the PQG Lagrangian here since it requires a good understanding of GR and mathematical machinery outside the scope of this work. The relevant Feynman rules for gravitational fermion scattering can be found in Appendix A and are presented without derivation. A thorough discussion on the derivation of the gravity-matter Lagrangian in PQG can be found in [1]. Nonetheless, we will discuss two important theoretical aspects of PQG. The first one is that gravitons are spin-2 bosons since they arise from a tensor field  $h_{\mu\nu}$ . On the other hand, photons, which arise from the vector potential  $A_\mu$ , are spin-1 bosons. One interesting property of spin-2 particles is that

the exchange of a spin-2 boson leads always to an attractive potential, this is consistent with our notion of Newtonian gravity being always an attractive force. The second important aspect of PQG is its gauge invariance. PQG is invariant under local space-time transformations,  $x^\mu \rightarrow x^\mu + \lambda^\mu(x)$ , also known as general coordinate transformation. By Noether's theorem, every symmetry is associated with a conserved current, which in the case of PQG is the energy-momentum tensor  $T_{\mu\nu}$ . This means that the conserved charge in PQG is energy and momentum.

## 4.2 Mass singularities in the gravitational electron scattering

In this section, we will study the gravitational equivalent of the electron scattering  $xe^- \rightarrow xe^-$  studied in subsection 2.3. The Feynman diagram for this process is the same as the one in Figure 2, with the photon line replaced by a graviton line. Using the Feynman rules in Appendix A, we find that up to the first two leading orders in the gravitational coupling constant  $\kappa$ , the Feynman diagrams relevant for the electron scattering are the same as in QED - Figure 1 - with every photon line replaced by a graviton line.

By looking at the equations for a fermion-graviton vertex and for a graviton propagator - Eq. A.2 and Eq. A.8 - we can see that the only source of singularities in the tree level diagram arises from the term  $\frac{1}{p^2}$  in the graviton propagator. We came across a similar singularity in QED for the tree level diagram of the electron scattering - see Eq. 2.8 - and concluded that such divergence did not correspond to a mass singularity. By the same argument, we can conclude that the tree level gravitational electron scattering is free of mass singularities. The exact numerical value of the matrix element for the tree level diagram will not be relevant for this work, all we need to know is that it contains no mass singularities. Henceforth, we will denote the matrix element for the tree level gravitational scattering by  $A_g$ .

Instead of repeating the calculation for all the non-radiative corrections - diagrams B, C, and D - and the real radiation diagrams - Figure 5 - a similar approach to the one taken in subsection 3.4 will be followed. That is, we will see how attaching a soft graviton to an external leg factorizes into a kinematic factor times the tree level diagram  $A_g$  and then use this result to treat real and virtual corrections individually.

Using the Feynman rules in Appendix A, the expression for attaching a soft graviton with momentum  $k$  to an outgoing external electron leg with momentum  $p'_1 + q$  is given by:

$$\bar{u}(p'_1) \frac{-\kappa}{8} [2\eta_{\mu\nu}(2p'_1 + \not{k} - 2m) - (2p'_1 + k)_\mu \gamma_\nu - \gamma_\mu (2p'_1 + k)_\nu] \frac{(\not{p}'_1 + \not{k}) + m}{(p'_1 + k)^2 - m^2 - i\epsilon} \mathcal{A}_0, \quad (4.3)$$

where  $\mathcal{A}_0$  is defined such that  $\bar{u}(p'_1)\mathcal{A}_0 = A_g$ . In subsection C.3, we show how in the soft graviton limit, the above expression simplifies to:

$$\left(\frac{\kappa}{2}\right) \left[ \frac{p'_{1,\mu} p'_{1,\nu}}{p'_1 \cdot k} \right] A_g. \quad (4.4)$$

The Lorentz indices  $\mu, \nu$  in the above expression are contracted with a graviton propagator if the graviton is virtual, or with a tensor-polarization sum, if the graviton is real. Neglecting the coupling constants, we can compare this expression to Eq. 3.2 and note that the eikonal factors of soft gravitons and soft photons are almost identical. In fact, the expressions only differ by the extra factor of  $p'_{1,\nu}$  in the numerator of the graviton. As we shall see later, this extra momentum factor will be responsible for the absence of collinear singularities in the final cross-section of the gravitational electron scattering.

Now, repeating the method from subsection 3.4, we want to consider attaching  $n$  soft gravitons to an external leg. The proof by induction in subsection 3.4 applies also to gravitons - just replace  $p'^{(n)}$  by  $p'_{1,\mu} p'_{1,\nu}$  - thus, we find that after summing over all the different permutations of attached gravitons, the factor obtained after attaching  $n$  soft gravitons to the outgoing external leg is given by:

$$y = \left(\frac{\kappa}{2}\right)^n \left(\frac{p'_{1,\mu} p'_{1,\nu}}{p'_1 \cdot k_1}\right) \left(\frac{p'_{1,\mu} p'_{1,\nu}}{p'_1 \cdot k_2}\right) \cdots \left(\frac{p'_{1,\mu} p'_{1,\nu}}{p'_1 \cdot k_n}\right) A. \quad (4.5)$$

By adding a minus sign inside each parenthesis in the above expression, we find the factor for attaching  $n$  soft gravitons to the incoming external leg, with momentum  $p_1$ . Thus, attaching  $n$  soft gravitons to either external leg and summing over all possible permutations gives:

$$Y = A_g \left(\frac{\kappa}{2}\right)^n \left(\frac{p'_{1,\mu} p'_{1,\nu}}{p'_1 \cdot k_1} - \frac{p_{1,\mu} p_{1,\nu}}{p_1 \cdot k_1}\right) \left(\frac{p'_{1,\mu} p'_{1,\nu}}{p'_1 \cdot k_2} - \frac{p_{1,\mu} p_{1,\nu}}{p_1 \cdot k_2}\right) \cdots \left(\frac{p'_{1,\mu} p'_{1,\nu}}{p'_1 \cdot k_n} - \frac{p_{1,\mu} p_{1,\nu}}{p_1 \cdot k_n}\right). \quad (4.6)$$

Now, we want to consider the matrix element for a scattering containing  $n$  virtual graviton loops. We begin by constructing a single graviton virtual loop by setting  $k_i = -k_j$ , inserting a graviton propagator  $G^{\mu\nu\alpha\beta}(p)$  - given by Eq. A.8 - and integrating over the 4-momentum of the soft graviton:

$$Y_{virtual} = \left(\frac{\kappa}{2}\right)^2 \int \frac{d^4 k}{(2\pi)^4} \left(\frac{p'_{1,\mu} p'_{1,\nu}}{p'_1 \cdot k_1} - \frac{p_{1,\mu} p_{1,\nu}}{p_1 \cdot k_1}\right) G^{\mu\nu\alpha\beta}(p) \left(-\frac{p'_{1,\alpha} p'_{1,\beta}}{p'_1 \cdot k_1} + \frac{p_{1,\alpha} p_{1,\beta}}{p_1 \cdot k_1}\right). \quad (4.7)$$

Since the graviton propagator  $G^{\mu\nu\alpha\beta}(p)$  contains only metric tensors  $\eta$ , it is not difficult to show- either using symmetry arguments or a long but simple calculation - that the above integral simplifies to:

$$Y_{virtual} = -i \left(\frac{\kappa}{2}\right)^2 \int \frac{d^4 k}{(2\pi)^4} \frac{1}{(k^2)} \left(\frac{2(p_1 \cdot p'_1)^2 - p_1^2 p_1'^2}{(p'_1 \cdot k)(p_1 \cdot k)} - \frac{(p_1')^2}{2(p'_1 \cdot k)^2} - \frac{(p_1)^2}{2(p_1 \cdot k)^2}\right), \quad (4.8)$$

where the factors of  $i\epsilon$  have been omitted for the sake of readability. Attaching  $n$  virtual loops to a tree level diagram will give  $n$  factors like  $Y_{virtual}$ . Multiplying by  $\frac{1}{2^n n!}$  to prevent over-counting, and summing over all diagrams containing up to  $n$  virtual graviton loops, the matrix element for a scattering with an arbitrary number of virtual loops is given by:

$$\mathcal{W}_{virtual} \stackrel{n \rightarrow \infty}{=} A_g \exp\left(\frac{Y_{virtual}}{2}\right), \quad (4.9)$$

$$\Rightarrow |\mathcal{W}_{virtual}|^2 = |A_g|^2 \exp [\operatorname{Re}(Y_{virtual})]. \quad (4.10)$$

In subsection D.3, it is shown that the real part of  $Y_{virtual}$  is given by:

$$\operatorname{Re}(Y_{virtual}) = -\frac{\kappa^2}{8(2\pi)^2} \ln \left( \frac{\Lambda}{|\mathbf{k}_{min}|} \right) g(\beta). \quad (4.11)$$

Inserting this result in Eq. 4.10 gives:

$$|\mathcal{W}_{virtual}|^2 = |A_g|^2 \left( \frac{|\mathbf{k}_{min}|}{\Lambda} \right)^{\frac{\kappa^2}{8(2\pi)^2} g(\beta)}, \quad (4.12)$$

where  $g(\beta)$ , with  $\beta$  given by Eq. 2.29, is defined as follows:

$$g(\beta) = \left[ \frac{1}{2} m_1 m_1 \frac{1 + \beta^2}{\beta \sqrt{1 - \beta^2}} \ln \left( \frac{1 + \beta}{1 - \beta} \right) - \frac{m_1^2}{2} - \frac{m_1^2}{2} \right]. \quad (4.13)$$

Now, we want to consider a scattering with the emission of  $m$  real soft gravitons. The matrix element squared of this process is obtained by inserting a graviton polarization tensor  $h_{\mu\nu}^*$  inside each parenthesis in Eq. 4.5, multiplying by its complex conjugate, summing over graviton polarizations and integrating over the on-shell momenta of the final gravitons:

$$|\mathcal{W}_{real}^{(m)}|^2 = |A_g|^2 \int d\mathcal{K} \prod_1^m \frac{\kappa^2}{(2\pi)^3 8 |\mathbf{k}_m|} \Psi(p_1, p'_1)_m, \quad (4.14)$$

where  $\Psi(p_1, p'_1)_m$  is defined as:

$$\Psi_m = \left( \frac{p'_{1,\mu} p'_{1,\nu} \Gamma p'_{1,\alpha} p'_{1,\beta}}{(p'_1 \cdot k_m)^2} - \frac{p'_{1,\mu} p'_{1,\nu} \Gamma p_{1,\alpha} p_{1,\beta}}{(p'_1 \cdot k_m)(p_1 \cdot k_m)} - \frac{p_{1,\mu} p_{1,\nu} \Gamma p'_{1,\alpha} p'_{1,\beta}}{(p'_1 \cdot k_m)(p_1 \cdot k_m)} + \frac{p_{1,\mu} p_{1,\nu} \Gamma p'_{1,\alpha} p'_{1,\beta}}{(p_1 \cdot k_m)^2} \right).$$

In the above expression,  $\Gamma$  is the graviton polarization sum. Since the graviton polarization tensor  $h_{\mu\nu}$  is a symmetric tensor, it can be written as a product of spin-one polarization vectors  $h^{\mu\nu} = \epsilon^\mu \epsilon^\nu$ . Moreover, the gauge invariance of PQG imposes the condition that the spin-one polarization vectors  $\epsilon^\mu$  and  $\epsilon^\nu$  must be transverse to the graviton momentum  $k$  and to each other [1]. This transverse-polarization property allows us to replace the spin-one polarization sums by metric tensors  $\eta$ . Thus:

$$\Gamma = \sum h_{\mu\nu}^* h_{\alpha\beta} = \sum \epsilon_\mu^* \epsilon_\nu^* \epsilon_\alpha \epsilon_\beta \rightarrow -\frac{1}{2} (\eta^{\mu\alpha} \eta^{\nu\beta} + \eta^{\mu\beta} \eta^{\nu\alpha} - \eta^{\mu\nu} \eta^{\alpha\beta}). \quad (4.15)$$

Substituting Eq. 4.15 in Eq. 4.14 and performing the tensor contractions gives:

$$|\mathcal{W}_{real}^{(m)}|^2 = |A_g|^2 \int d\mathcal{K} \prod_1^m \frac{\kappa^2}{(2\pi)^3 8 |\mathbf{k}_m|} \left( \frac{2(p_1 \cdot p'_1)^2 - p_1^2 p_1'^2}{(p'_1 \cdot k)(p_1 \cdot k)} - \frac{(p_1'^2)^2}{2(p'_1 \cdot k)^2} - \frac{(p_1^2)^2}{2(p_1 \cdot k)^2} \right). \quad (4.16)$$

The above integrals can be solved noting that the on-shell condition,  $\delta(k^0 = |\mathbf{k}|)$ , turns the above integrals into  $m$  integrals of the form Eq. D.9. Using the results from subsection D.3, the  $d\mathcal{K}$  integral in Eq. 4.16 gives:

$$|\mathcal{W}_{real}^{(m)}|^2 = \frac{|A_g|^2}{m!} \left[ \frac{\kappa^2}{8(2\pi)^2} \ln \left( \frac{E_t}{|\mathbf{k}_{min}|} \right) g(\beta) \right]^m, \quad (4.17)$$

where we multiplied by  $m!$  to avoid over-counting since there are  $m$  gravitons - bosons - in the final state. Summing the contribution of all diagrams containing up to  $m$  real soft gravitons gives:

$$|\mathcal{W}_{real}| \stackrel{m \rightarrow \infty}{=} |A_g|^2 \left( \frac{E_t}{|\mathbf{k}_{min}|} \right)^{\frac{\kappa^2}{8(2\pi)^2} g(\beta)}. \quad (4.18)$$

Finally, using Eq. 4.10 and Eq. 4.18, the matrix element squared of a gravitational electron scattering containing an arbitrary number of soft virtual and soft real gravitons can be written as:

$$|\mathcal{W}|^2 = |A_g|^2 \left( \frac{E_t}{\Lambda} \right)^{\frac{\kappa^2}{8(2\pi)^2} g(\beta)}. \quad (4.19)$$

Similar to the result we found in QED, a process containing an arbitrary number of soft gravitons - real or virtual - factorizes into the tree level diagram  $A_g$ , times a factor which is independent of the minimum graviton energy  $|\mathbf{k}_{min}|$ . Therefore, the above matrix element is IR finite. Now, we can study the collinear behaviour by letting the mass  $m_1$  of the external leg  $p'_1$  go to zero while fixing its momentum  $\mathbf{p}'_1$  constant. Taylor expanding  $g(\beta)$  to second order in  $m_1^2$  gives:

$$g(\beta) \approx (p'_1 \cdot p_1) \ln(m_1^2 m_1^2) - \frac{m_1^2 m_1^2}{(p'_1 \cdot p_1)} \ln(m_1^2 m_1^2) + \mathcal{O}(m_1^6). \quad (4.20)$$

Due to the factor  $m_1^2$  behind the logarithm, the second term in the above expression goes to zero in the limit  $m_1 \rightarrow 0$ . Moreover, Lorentz invariance for gravitons - conservation of the energy-momentum tensor - implies momentum conservation, which in the soft graviton limit allows us to make the approximation  $p'_1 \cdot p_1 \approx p_1'^2$ . This means that the first term also goes to zero in the limit  $m_1 \rightarrow 0$ . Therefore, the matrix element squared for an electron scattering containing an arbitrary number of real and virtual soft gravitons is finite both in the IR and the collinear limit. The factors of  $m_1^2$ , and  $p_1'^2$  that appear behind the logarithms in the above equation, occur in PQG but not on QED due to the extra factor of  $p$  in the PQG eikonal factor, see Eq. 4.4.



## 5 Conclusion

In subsection 2.3, we saw that if only the non-radiative diagrams are considered, the cross-section of the electron scattering is divergent both in the soft and collinear limits. From Eq. 2.27 and Eq. 2.28, the physical origin of the mass singularities became clear; soft singularities occur if the photon energy vanishes, while collinear singularities occur if a massless electron emits a collinear photon. In subsection 3.1, we found that scatterings with real radiation contain the same type of mass singularities as those in the non-radiative diagrams. We discussed why, to a detector with finite energy resolution  $E_t$ , scatterings with real radiation photons with energy less than  $E_t$  are degenerate to scatterings with no real radiation. The S-matrix formalism states that to calculate a scattering amplitude, we must sum over all degenerate final states. Thus, non-radiative diagrams, as well as radiative diagrams, must be included when computing the scattering amplitude. We saw that by doing this, the cross-section of the scattering process became IR (soft) regular. A more thorough calculation would have led to the same conclusion regarding collinear singularities. That is, mass singularities cancel when the contribution of real radiation diagrams is included in the cross-section[5][6].

Given that the cross-section of a process is an observable, we expect the cancellation of mass singularities to occur not only to first order but to all orders. In subsection 3.4, we showed how IR (soft) singularities in QED cancel to all orders if real and virtual corrections are included. Moreover, we showed that the scattering cross-section was independent of the photon's lowest energy and was determined by the detector's threshold resolution  $E_t$ . However, there was a complication with the proof in subsection 3.4, the collinear singularity was still present since  $f(\beta)$  was divergent if the mass of one of the external electrons was sent to zero while fixing its spatial momentum constant. Even though there are no massless charged particles in QED, we expect collinear singularities to cancel, since in experiments where  $Q \gg m_e$ , the contributions from the divergent behaviour of collinear singularities become important. A proof of the cancellation of collinear singularities to all orders can be achieved but requires treatment beyond the soft photon approximation [5]. This last point is where a significant difference between the structure of mass singularities in QED and PQG scatterings was found.

In subsection 4.2, we showed the cancellation of IR (soft) singularities to all orders in a gravitational electron scattering process and arrived at a similar result as in QED. That is, we showed that the cross-section of a process with an arbitrary number of real and virtual soft gravitons is IR finite. More importantly, we found that the cross-section was also free of collinear singularities since  $g(\beta)$  goes to zero in the electron massless limit. The cancellation of both soft and collinear singularities in the soft graviton approximation - but not in the soft photon approximation - points towards a fundamental difference between the structure of QED and PQG. It was also shown that the eikonal factorization of PQG was quite similar to that of QED.

The eikonal factor - Eq. 3.2 and Eq. 4.4 - can be separated in two parts. The factor of  $\frac{p}{p \cdot k}$  is a kinematic factor, independent of the gauge theory, while the rest is a factor related to the “charge coupling” of the particular gauge theory. In QED, the coupling of a photon to a fermion is independent of the momenta of either particle. This is not the case for PQG, where the momentum appears in the coupling vertex of a graviton to a fermion. In QED, the “charge coupling” factor  $e$  is given by the electric charge of the fermion to which the photon couples to, while for PQG, the “charge coupling” factor is  $\frac{k}{2}p$ . The appearance of a momentum factor in the “charge coupling” part of the eikonal factor is a consequence of the role that momentum plays as a “conserved current” in PQG. By Noether’s theorem, the gauge invariance of QED leads to the conservation of electric charge. Similarly, the gauge invariance of PQG under general coordinate transformations implies the conservation of energy and momentum. Hence, momentum plays the same role in PQG as electric charge plays in QED, which explains the presence of momentum factors in the “charge coupling” part of the gravitational eikonal factor. The extra momentum factor in the eikonal factor of PQG leads to additional factors, which are responsible for the absence of collinear singularities in the massless electron limit.

The structural differences between QED and PQG scatterings discussed above indicate that there could be a more fundamental difference in the way that the graviton tensor field couples to matter. Here, only an example of a scattering process was studied, where only boson-fermion vertexes were considered. Even in this simplified scenario, a structural difference between QED and PQG was found. Namely, in PQG, the coupling of gravitons to fermions vanishes in the massless fermion limit, leading to collinear finite cross-sections, even in the soft graviton approximation.

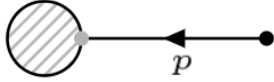
By studying more general graviton interactions, it may be possible to extract more fundamental and general properties of PQG and its singularity structure. However, the diagrammatic structure of PQG is incredibly complicated, since the vertices of gravitons to other particles of the SM and other gravitons [1] become almost impossible to deal with by hand. Thus, future treatments of the subject should avoid a diagrammatic approach, and instead should focus on more fundamental properties of the theory, such as the scaling of the fields [11].

We conclude this section by mentioning why, throughout this work, QED and PQG scatterings were treated as separate processes. This simplification is justified by the enormous difference between the universal gravitational constant  $G$  and the EM fine-structure constant  $\alpha$ , which in natural units is roughly  $1 : 10^{35}$ . Thus, gravity will not significantly contribute to the electron scattering process discussed in subsection 2.3 and section 3.

# A Feynman rules

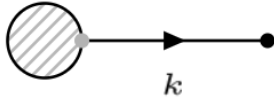
## A.1 Quantum electrodynamics

Here, some relevant Feynman rules for QED are listed without derivation. For a detailed discussion on the derivation of these rules see [3].



External Fermion Leg:

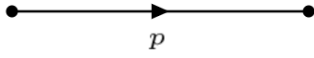
$$= u^s(p) = u(p, s), \tag{A.1}$$



External Antifermion Leg:

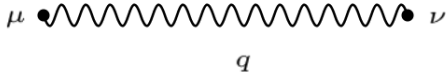
$$= \bar{u}^s(k) = \bar{u}(k, s), \tag{A.2}$$

where the terms inside the parenthesis  $(p, s)$  -  $(k, s)$  - correspond to the 4-momentum and spin of the fermion - antifermion- respectively.



Fermion propagator:

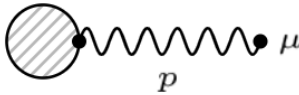
$$= \frac{i(\not{p} + m)}{p^2 - m^2 + i\epsilon}, \tag{A.3}$$



Photon propagator:

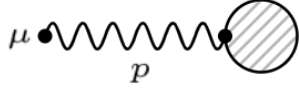
$$= \frac{-i}{q^2} \left[ \eta_{\mu\nu} + n \frac{q_\mu q_\nu}{q^2} \right], \tag{A.4}$$

where  $n$  is a gauge-fixing parameter. Two common choices are the Landau gauge with  $n = -1$  and the Feynman gauge with  $n = 0$ . If the gauge parameter is not explicitly defined, Feynman gauge is assumed.



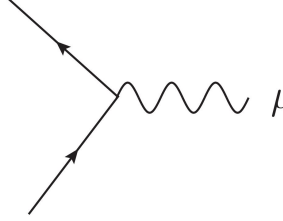
External Photon Leg:

$$= \epsilon_\mu = \epsilon(p, \lambda), \tag{A.5}$$



$$= \epsilon_\mu^* = \epsilon^*(p, \lambda), \quad (\text{A.6})$$

where  $\epsilon(p, \lambda)$  and  $\epsilon^*(p, \lambda)$ , with  $\lambda = \pm 1$ , represent the polarization vectors of initial and final photons respectively.

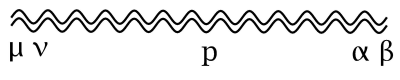


Fermion-Fermion-Photon Vertex:

$$= -ie\gamma^\mu. \quad (\text{A.7})$$

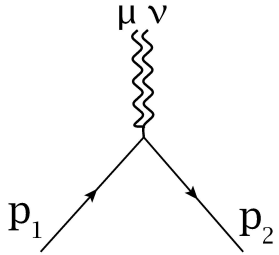
## A.2 Perturbative quantum gravity

Here, we provide a list of the Feynman rules for PQG relevant for this work. For a more detailed and complete list of the Feynman rules for PQG see [1].



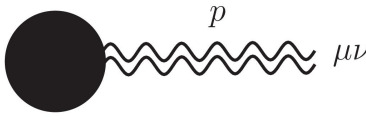
Graviton Propagator:

$$= \frac{i}{2} \frac{\eta^{\mu\alpha}\eta^{\nu\beta} + \eta^{\mu\beta}\eta^{\nu\alpha} - \eta^{\mu\nu}\eta^{\alpha\beta}}{p^2}, \quad (\text{A.8})$$



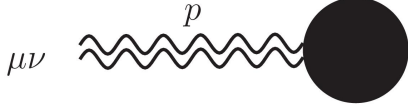
Fermion-Fermion-Graviton Vertex:

$$= \frac{i}{8} \kappa [2\eta_{\mu\nu} (\not{p}_1 + \not{p}_2 - 2m) - (p_1 + p_2)_\mu \gamma_\nu - \gamma_\mu (p_1 + p_2)_\nu], \quad (\text{A.9})$$



External Graviton Leg:

$$= h_{\mu\nu}(p) = \epsilon_\mu(p)\epsilon_\nu(p), \quad (\text{A.10})$$



$$= h_{\mu\nu}^*(p) = \epsilon_\mu^*(p)\epsilon_\nu^*(p), \quad (\text{A.11})$$

where  $h_{\mu\nu}(p)$  and  $h_{\mu\nu}^*(p)$  represent the polarization tensors of initial and final gravitons respectively.

## B Numerator algebra

In this appendix we provide a list of identities used to simplify the numerators of the different expressions throughout this work. The identities here are provided without a proof, for a derivation of these identities the reader is referred to [3][4][5].

The free propagating spinor  $u^s(p)$  obeys the Dirac equation:

$$(\not{p} - m)u^s(p) = \bar{u}^s(p)(\not{p} - m) = 0. \quad (\text{B.1})$$

Spinors also satisfy the following completeness relation for spin sums:

$$\sum_s u^s(p)\bar{u}^s(p) = \not{p} + m. \quad (\text{B.2})$$

Using the above identity, a very useful formula for spin sums can be proven:

$$\sum_{s,s'} \bar{v}_a^{s'}(p')\gamma_{ab}^\mu u_b^s(p)\bar{u}_c^s\gamma_{cd}^\nu v_d^{s'}(p') = \text{tr}[(\not{p}' - m)\gamma^\mu(\not{p} + m)\gamma^\nu]. \quad (\text{B.3})$$

It can be shown by explicit calculation that Dirac matrices satisfy the following identities:

$$\{\gamma^\mu, \gamma^\nu\} = 2\eta^{\mu\nu} \quad ; \quad \gamma^\mu\gamma_\mu = 4. \quad (\text{B.4})$$

## C Supplementary calculations

### C.1 Tree level diagram QED

Here, we show how the matrix element squared of the tree level electron scattering process in Eq. 2.8 can be obtained from Eq. 2.7. Rearranging and contracting one of the gamma matrices in Eq. 2.7, the amplitude for the process becomes:

$$A = \frac{ie^2}{q^2} (\bar{u}(p'_1, s'_1)\gamma^\mu u(p_1, s_1)) (\bar{u}(p'_2, s'_2)\gamma_\mu u(p_2, s_2)). \quad (\text{C.1})$$

Noting that  $(\bar{v}\gamma^\mu u)^* = \bar{u}\gamma^\mu v$ , the complex conjugate of the above expression is given by:

$$A^* = \frac{-ie^2}{q^2} (\bar{u}(p_1, s_1)\gamma^\nu u(p'_1, s'_1)) (\bar{u}(p_2, s_2)\gamma_\nu u(p'_2, s'_2)). \quad (\text{C.2})$$

The unpolarized matrix element squared can then be obtained combining the above expressions:

$$|A|_{unp}^2 = \frac{e^4}{q^4} [\bar{u}(p'_1, s'_1)\gamma^\mu u(p_1, s_1)\bar{u}(p_1, s_1)\gamma^\nu u(p'_1, s'_1)] [\bar{u}(p'_2, s'_2)\gamma_\mu u(p_2, s_2)\bar{u}(p_2, s_2)\gamma_\nu u(p'_2, s'_2)].$$

Finally, assuming unpolarized incoming particles, we must average over incoming spins  $(s_1, s_2)$  and sum over final spins  $(s'_1, s'_2)$ .

$$|A|^2 = \frac{1}{2} \sum_{s_1} \frac{1}{2} \sum_{s_2} \sum_{s'_1} \sum_{s'_2} |A|_{unp}^2. \quad (\text{C.3})$$

The above sums can be performed using the spin sum identities in Appendix B. Using the massless electron approximation, Eq. C.3 becomes:

$$|A|^2 = \frac{e^4}{4q^4} \text{tr}[\not{p}'_1\gamma^\mu + \not{p}_1\gamma^\nu] \text{tr}[(\not{p}'_2 + m)\gamma_\mu + (\not{p}_2 + m)\gamma_\nu], \quad (\text{C.4})$$

where  $m$  is the mass of the massive particle. Using trace identities for gamma matrices, the above equation simplifies as follows:

$$|A|^2 = \frac{8e^4}{q^4} [(p_1 \cdot p'_2)(p'_1 \cdot p_2) + (p_1 \cdot p_2)(p'_1 \cdot p'_2) - m^2(p_1 \cdot p'_1)], \quad (\text{C.5})$$

which is the desired equation.

## C.2 Imaginary factors in Feynman propagators

Imaginary parts of loop amplitudes come from virtual particles going on-shell.

*Proof.* To prove this statement, we will assume that Feynman propagators are analytic functions and can be analytically continued to the whole complex plane. Hence, the discontinuity of a propagator  $f(s)$ , across any branch cut it may have, is proportional to its imaginary part [4]. If the propagator contains a branch cut in the real axis at  $s$ , then:

$$\text{Discontinuity}(f(s)) = 2i\text{Im}(f(s + i\epsilon)). \quad (\text{C.6})$$

Let us illustrate the use of this result by computing the imaginary part of a photon propagator:

$$\text{Im}\left(\frac{1}{k^2 + i\epsilon}\right) = \frac{1}{2i}\text{Discontinuity} = \frac{1}{2i}\left(\frac{1}{k^2 + i\epsilon} - \frac{1}{k^2 - i\epsilon}\right) = \frac{-\epsilon}{(k^2)^2 + \epsilon^2}. \quad (\text{C.7})$$

The above expression vanishes in the limit  $\epsilon \rightarrow 0$ , except at the point  $k^2 = 0$ . Integrating  $k^2$  in the above expression for  $k^2 > 0$  gives:

$$\int_0^\infty dk^2 \frac{-\epsilon}{(k^2)^2 + \epsilon^2} = -\pi, \quad (\text{C.8})$$

$$\Rightarrow \text{Im} \left( \frac{1}{k^2 + i\epsilon} \right) = -\pi \delta(k^2). \quad (\text{C.9})$$

Hence, the imaginary part of a massless propagator vanishes except when the particle goes on-shell.  $\square$

### C.3 Soft graviton simplification

Here, we show how Eq. 4.3 simplifies to Eq. 4.4 in the soft graviton limit. First, let us do some algebra in the numerator  $N$  to simplify it:

$$N = -\kappa \bar{u}(p'_1) [2\eta_{\mu\nu}(2p'_1 + k - 2m_1) - (2p'_1 + k)_\mu \gamma_\nu - \gamma_\mu(2p'_1 + k)_\nu] (\not{p}'_1 + \not{k} + m_1) \mathcal{A}_0. \quad (\text{C.1})$$

In the soft graviton approximation we can drop the terms  $k$  in the numerator:

$$N = -\kappa \bar{u}(p'_1) [2\eta_{\mu\nu}(2p'_1 - 2m_1) - (2p'_1)_\mu \gamma_\nu - \gamma_\mu(2p'_1)_\nu] (\not{p}'_1 + m_1) \mathcal{A}_0. \quad (\text{C.2})$$

The first term inside the squared brackets cancels when multiplied by the numerator of the electron propagator since the outgoing electron is on-shell, i.e.  $p_1'^2 = m_1^2$ . The other two terms can be rewritten as:

$$N = \kappa [(2p'_1)_\mu \bar{u}(p'_1) \gamma_\nu (\not{p}'_1 + m_1) + \bar{u}(p'_1) \gamma_\mu (\not{p}'_1 + m_1) (2p + q)_\nu] \mathcal{A}_0. \quad (\text{C.3})$$

Using the commutation relations for the Dirac matrices, and the identities in Appendix B, the above expression simplifies to:

$$N = 8\kappa [p'_{1,\mu} p'_{1,\nu}] \bar{u}(p'_1) \mathcal{A}_0 = 8\kappa [p'_{1,\mu} p'_{1,\nu}] A_g. \quad (\text{C.4})$$

On the other hand, the denominator simply becomes:

$$8((p'_1)^2 + 2p'_1 \cdot k + k^2 - m_1^2) = 16(p'_1 \cdot k). \quad (\text{C.5})$$

Combining the last two expressions gives the desired expression in Eq. 4.4.

## D Integral evaluation

In this appendix, we evaluate the most important integrals that appeared in the calculations:

**D.1 Eq. 2.24**

$$I_{loop} = \frac{ie^2}{(2\pi)^4} \int d^4k \frac{1}{(k^2 + i\epsilon)(p \cdot k + i\epsilon)}. \quad (D.1)$$

We are interested in the real part of the above integral. This integral can be evaluated by contour integration of  $k^0$  in the complex plane. The integrand is analytic in  $k^0$  except at three poles;

$$k^0 = |\mathbf{k}| - i\epsilon, \quad k^0 = -|\mathbf{k}| + i\epsilon, \quad \text{and} \quad k^0 = \frac{\mathbf{k} \cdot \mathbf{p}}{p^0} - i\epsilon.$$

By closing the integration in the upper-plane with a large semi-circle, we avoid the two poles in the lower-plane. Thus, the integral only gets a contribution from the pole at  $k^0 = -|\mathbf{k}| + i\epsilon$ . This pole gives a factor of  $\frac{-i\pi}{|\mathbf{k}|}$  for the  $k^0$  integral. After performing the  $k^0$  integral, Eq. 2.24 becomes:

$$I_{loop} = \frac{e^2\pi}{(2\pi)^4} \int_{|\mathbf{k}_{min}|}^{\Lambda} \frac{d^3k}{|\mathbf{k}|^2(p^0 - \mathbf{p} \cdot \hat{\mathbf{k}})} = \frac{\alpha}{(2\pi)^2} \int_{|\mathbf{k}_{min}|}^{\Lambda} d|\mathbf{k}| \int \frac{\Omega_{\hat{\mathbf{k}}}}{(p^0 - \mathbf{p} \cdot \hat{\mathbf{k}})}. \quad (D.2)$$

The above integral is purely real.

**D.2 Eq. 2.26**

$$V_f = \frac{-ie^2}{(2\pi)^4} \left[ \int d^4k \frac{p'_1 \cdot p_1}{(p'_1 \cdot k + i\epsilon)(k^2 + i\epsilon)(p_1 \cdot k + i\epsilon)} - \frac{p_1^2}{(k^2 + i\epsilon)(p_1 \cdot k + i\epsilon)^2} \right]. \quad (D.3)$$

Again, we are interested in the real part of the above integral. Similar to the previous integral, we will evaluate the real part of Eq. 2.28 by first integrating  $k^0$  using a contour integral. Let us first look at the first term in the integrand. The integrand is analytic except at four poles;

$$k^0 = |\mathbf{k}| - i\epsilon, \quad k^0 = -|\mathbf{k}| + i\epsilon, \quad k^0 = \frac{\mathbf{k} \cdot \mathbf{p}'_1}{p_1'^0} - i\epsilon, \quad \text{and} \quad k^0 = \frac{\mathbf{k} \cdot \mathbf{p}_1}{p_1^0} - i\epsilon.$$

Again, by closing the contour with a large semi-circle in the upper-plane, we get a contribution to the integral only from the pole at  $k^0 = -|\mathbf{k}| + i\epsilon$ , which again gives a factor of  $\frac{-i\pi}{|\mathbf{k}|}$ . After performing the  $k^0$  integral, Eq. 2.28 becomes:

$$\begin{aligned} V_f^{(1)} &= \frac{-e^2\pi}{(2\pi)^4} \int_{|\mathbf{k}_{min}|}^{\Lambda} d^3k \frac{p'_1 \cdot p_1}{|\mathbf{k}|^3(p_1'^0 - \mathbf{p}'_1 \cdot \hat{\mathbf{k}})(p_1^0 - \mathbf{p}_1 \cdot \hat{\mathbf{k}})}, \\ &\Rightarrow \frac{-\alpha}{(2\pi)^3} \ln \left( \frac{\Lambda}{|\mathbf{k}_{min}|} \right) \int \Omega_{\hat{\mathbf{k}}} \frac{p'_1 \cdot p_1}{(p_1'^0 - \mathbf{p}'_1 \cdot \hat{\mathbf{k}})(p_1^0 - \mathbf{p}_1 \cdot \hat{\mathbf{k}})}. \end{aligned} \quad (D.4)$$



The  $\hat{\mathbf{k}}$ -angular integral is a relatively common integral in scattering particle physics, whose analytic solution is [5]:

$$\int \Omega_{\hat{\mathbf{k}}} \frac{p'_1 \cdot p_1}{(p_1'^0 - \mathbf{p}'_1 \cdot \hat{\mathbf{k}})(p_1^0 - \mathbf{p}_1 \cdot \hat{\mathbf{k}})} = 2\pi \left( \frac{1}{2\beta} \ln \left( \frac{1+\beta}{1-\beta} \right) \right), \quad (\text{D.5})$$

where  $\beta$  is the relative velocity between the incoming and outgoing electron, given by Eq. 2.29.

The second part of the integrand in Eq. D.3 can be solved again by contour integration, noting that the integration has the same poles as the integral in subsection D.1. Integrating  $k^0$  the same way as in subsection D.1, gives the same contribution and the integral becomes:

$$\begin{aligned} V_f^{(2)} &= \frac{-\alpha}{(2\pi)^2} \int_{|\mathbf{k}_{min}|}^{\Lambda} \frac{d|\mathbf{k}|}{|\mathbf{k}|} \int \Omega_{\hat{\mathbf{k}}} \frac{p_1^2}{(p^0 - \mathbf{p} \cdot \hat{\mathbf{k}})^2}, \\ &\Rightarrow V_f^{(2)} = \frac{-\alpha}{2\pi} \ln \left( \frac{\Lambda}{|\mathbf{k}_{min}|} \right). \end{aligned} \quad (\text{D.6})$$

Finally, combining Eq. D.4 and Eq. D.6 gives:

$$V_f = \frac{-\alpha}{2\pi} \ln \left( \frac{\Lambda}{|\mathbf{k}_{min}|} \right) \left[ \frac{1}{2\beta} \ln \left( \frac{1+\beta}{1-\beta} \right) - 1 \right]. \quad (\text{D.7})$$

The integral above is purely real.

### D.3 Eq. 4.8

$$Y_{virtual} = -i \left( \frac{\kappa}{2} \right)^2 \int \frac{d^4k}{(2\pi)^4} \frac{1}{(k^2)} \left( \frac{2(p_1 \cdot p'_1)^2 - p_1^2 p_1'^2}{(p'_1 \cdot k)(p_1 \cdot k)} - \frac{(p_1')^2}{2(p'_1 \cdot k)^2} - \frac{(p_1)^2}{2(p_1 \cdot k)^2} \right). \quad (\text{D.8})$$

Note that in the above integral, the analytic form of the  $k^0$  integral is identical to the vertex function integral  $V_f$ , discussed in the previous section. That is, the poles are the same, and by closing the contour upwards, only the pole at  $k^0 = -|\mathbf{k}| + i\epsilon$  contributes to the integral. After performing the  $k^0$  integral using the result from the previous section,  $Y_{virtual}$  becomes:

$$Y_{virtual} = - \left( \frac{\kappa^2}{8(2\pi)^3} \right) \ln \left( \frac{\Lambda}{|\mathbf{k}_{min}|} \right) \int \Omega_{\hat{\mathbf{k}}} \left( \frac{2(p_1 \cdot p'_1)^2 - p_1^2 p_1'^2}{(p'_1 \cdot \hat{\mathbf{k}})(p_1 \cdot \hat{\mathbf{k}})} - \frac{(p_1')^2}{2(p'_1 \cdot \hat{\mathbf{k}})^2} - \frac{(p_1)^2}{2(p_1 \cdot \hat{\mathbf{k}})^2} \right). \quad (\text{D.9})$$

The first  $\hat{\mathbf{k}}$ -angular integral is given by [8]:

$$2\pi \left[ \frac{1}{2} m_1 m_1 \frac{1+\beta^2}{\beta \sqrt{1-\beta^2}} \ln \left( \frac{1+\beta}{1-\beta} \right) \right]. \quad (\text{D.10})$$

The other two angular integrals are almost identical to the second angular integral of the vertex function  $V_f$ . The only difference is that the angular integrals here have an additional factor of  $p^2$  in the numerator, which by noting that the external electrons must be on-shell can be replaced by  $m^2$ . Thus, the second and third angular integrals above give:

$$2\pi \left( -\frac{m_1^2}{2} - \frac{m_1^2}{2} \right). \quad (\text{D.11})$$

Inserting Eq. D.10 and Eq. D.11 in Eq. D.9 gives:

$$Y_{virtual} = - \left( \frac{\kappa^2}{8(2\pi)^2} \right) \ln \left( \frac{\Lambda}{|\mathbf{k}_{min}|} \right) \left[ \frac{(m_1 m_1)(1 + \beta^2)}{2(\beta\sqrt{1 - \beta^2})} \ln \left( \frac{1 + \beta}{1 - \beta} \right) - \frac{m_1^2}{2} - \frac{m_1^2}{2} \right], \quad (\text{D.12})$$

which again, is purely real.

## References

- [1] S. Y. Choi, J. S. Shim, and H. S. Song, “Factorization and polarization in linearized gravity,” *Phys. Rev.*, vol. D51, pp. 2751–2769, 1995.
- [2] F. Bloch and A. Nordsieck, “Note on the radiation field of the electron,” *Phys. Rev.*, vol. 52, pp. 54–59, Jul 1937.
- [3] M. E. Peskin and D. V. Schroeder, *An Introduction to quantum field theory*. Reading, USA: Addison-Wesley, 1995.
- [4] M. D. Schwartz, *Quantum Field Theory and the Standard Model*. Cambridge University Press, 2014.
- [5] M. Bohm, A. Denner, and H. Joos, *Gauge theories of the strong and electroweak interaction*. Auflage, 2001.
- [6] T. Kinoshita, “Mass singularities of Feynman amplitudes,” *J. Math. Phys.*, vol. 3, pp. 650–677, 1962.
- [7] C. W. Bauer, S. Fleming, D. Pirjol, and I. W. Stewart, “An Effective field theory for collinear and soft gluons: Heavy to light decays,” *Phys. Rev. D*, vol. 63, p. 114020, 2001.
- [8] S. Weinberg, “Infrared photons and gravitons,” *Phys. Rev.*, vol. 140, pp. B516–B524, 1965.
- [9] T. D. Lee and M. Nauenberg, “Degenerate systems and mass singularities,” *Phys. Rev.*, vol. 133, pp. B1549–B1562, Mar 1964.
- [10] C. W. Misner, K. Thorne, and J. Wheeler, *Gravitation*. San Francisco: W. H. Freeman, 1973.
- [11] M. Beneke and G. Kirilin, “Soft-collinear gravity,” *JHEP*, vol. 09, p. 066, 2012.